

HE  
18.5  
.A38  
no. DOT-  
TSC-93-1

REPORT NO. DOT-TSC-93-1

DEPARTMENT OF  
TRANSPORTATION

JAN 18 1973

LIBRARY

# MODELING OF V/STOL NOISE IN CITY STREETS

RICHARD H. LYON  
LALIT PANDE  
WAYNE A. KINNEY  
DEPARTMENT OF MECHANICAL ENGINEERING  
MASSACHUSETTS INSTITUTE OF TECHNOLOGY  
CAMBRIDGE, MASS. 02139



U.S. International Transportation Exposition  
Dulles International Airport  
Washington, D.C.  
May 27-June 4, 1972



NOVEMBER 1971  
TECHNICAL REPORT

Availability is Unlimited. Document may be Released  
To the National Technical Information Service,  
Springfield, Virginia 22151, for Sale to the Public.

Prepared for:  
OFFICE OF NOISE ABATEMENT  
DEPARTMENT OF TRANSPORTATION  
WASHINGTON, D.C. 20591

The contents of this report reflect the views of the Massachusetts Institute of Technology, which is responsible for the facts and the accuracy of the data presented herein. The contents do not necessarily reflect the official views of the Department of Transportation. This report does not constitute a standard, specification, or regulation.

HE  
18.5  
.A38  
no.  
DOT-  
TSC-  
93-1

U.S. Transportation, Dept. of. Transportation Systems  
... 2 3  
Center.

DEPARTMENT OF  
TRANSPORTATION  
  
JAN 18 1973

1. Report No. DOT-TSC-93-1,		2. Government Accession No.		3. Recipient's Catalog No. LIBRARY	
4. Title and Subtitle ✓ ✓ MODELING OF V/STOL NOISE IN CITY STREETS,				5. Report Date 15 November 1971	
				6. Performing Organization Code	
7. Author(s) Richard H. Lyon, Lalit Pande, Wayne A. Kinney				8. Performing Organization Report No.	
9. Performing Organization Name and Address Department of Mechanical Engineering Massachusetts Institute of Technology Cambridge, Mass. 02139				10. Work Unit No. R-2519	
				11. Contract or Grant No. DOT-TSC-93	
12. Sponsoring Agency Name and Address Office of Noise Abatement Department of Transportation Washington, D.C. 20591				13. Type of Report and Period Covered Contractor Report	
				14. Sponsoring Agency Code	
15. Supplementary Notes					
16. Abstract The goals of this work were two-fold. First, to develop modeling techniques that will be helpful in studying a variety of noise propagation problems. These involve not only aircraft sources, but also surface traffic (automobiles, trucks, and rail vehicles) as well. The second and more narrow goal is the application of these modeling techniques to a specific problem, the propagation of V/STOL aircraft noise into an urban area.  Two particular flight-path-street-configuration situations were examined, using a 1:32 scale for the laboratory model. A steady-state aerodynamic noise source was used to simulate flyover noise. A second source for generating sound pulses was used for ray-tracing diagnoses.  The propagation effects of streets and buildings, which cause sound levels to differ from that in open flat terrain, are lumped together into a "Transmission Gain (TG)". A major part of the work reported here is the experimental evaluation of TG for various model configurations, flight paths, and microphone locations.					
17. Key Words • Noise levels • V/STOL noise • Noise propagation • Urban noise propagation			18. Distribution Statement Availability is Unlimited. Document may be Released To the National Technical Information Service, Springfield, Virginia 22151, for Sale to the Public.		
19. Security Classif. (of this report) UNCLASSIFIED		20. Security Classif. (of this page) UNCLASSIFIED		21. No. of Pages 49	22. Price



## Table of Contents

Table of Contents	i
List of Illustrations	ii
List of Tables	iv
I. Introduction	1
II. Scaling Laws and Modeling Techniques	4
III. Steady-State Experiments	18
IV. Transient Experiments	30
V. Discussion and Summary	38
References	49



## List of Illustrations

<u>Figure</u>	<u>Page</u>
1. Illustration of 4:1 scaling of dimensions and wavelength.	5
2. Air absorption under normal laboratory conditions.	8
3. Air absorption using dried air in laboratory.	8
4. Steady-state broad band noise source.	11
5. Spectrum of steady-state noise source, measured at 1 foot.	12
6. Spark gap transient sound source.	13
7. Energy spectrum of spark source in 1/3 octave bands.	14
8. Line-up of steady-state instrumentation.	16
9. Equipment line-up for transient experiments.	17
10. Model configuration for street overflight experiments.	19
11. Measured band levels and calculated open terrain band levels for same flyover.	22
12. The variation of Perceived Noise Level as a function of source position for flyover across a city street.	23
13. The variation of Perceived Noise Level as a function of source position for flyover across a city street.	24
14. Perceived Noise Level as a function of source position.	25
15. Perceived Noise Level as a function of source position for flyover of L-shaped street.	26
16. Perceived Noise Level as a function of source position for a longitudinal flyover.	27
17. Time pattern for sound pressure for position B.	31
18. Cross-section of model city block.	33
19. Time pattern of sound pressure for position F.	34
20. Time pattern of sound pressure for position B.	36
21. Time pattern of sound pressure for position F.	37
22. Measured value of sound pressure level at 1 foot.	41

23. Graph of $L_p$ vs. source position.	42
24. Combined graph of $L_p$ vs. source position for steady-state and transient sources.	43
25. Top view of L-shaped street model.	45
26. 1:64 scale model of urban area near STOL-port.	47

List of Tables

<u>Table</u>	<u>Page</u>
1. Summation procedure as used on the photograph for position A in the L-shaped street configuration.	40



## I. Introduction

The propagation of noise from aircraft on the ground and at low altitudes into an urban environment is a very complicated problem. At some places, the sound may be enhanced because of channeling of energy along the street in a duct-like fashion. At other locations, the sound may be diminished because buildings or other obstructions shield the observer from the source of noise. The purpose of the study reported here is the development of certain experimental tools that should help shed new light on the propagation of sound in these circumstances.

In a broader sense, the goals of this work are two-fold. First, we seek to develop modeling techniques that will be helpful in studying a variety of noise propagation problems. These involve not only aircraft noise sources, but surface traffic (automobiles, trucks, and rail vehicles) as well. The propagation situation may involve urban areas of highway designs with various land profiles. Whatever the situation, the sources, receivers, and signal processing techniques we have developed and will develop in the future should be useful.

The second and more narrow goal is the application of these modeling techniques to our particular problem, the propagation of V/STOL aircraft noise into an urban area. To this end, we have examined two particular flight part-street layout configurations, which are described in Section III. We have selected a 1:32 scale for the laboratory model. A steady-state aerodynamic noise source is used as a sound source for simulating flyover noise. A second source for generating sound pulses has also been used for diagnostic purposes. We shall have more to say about the use of these sources in Sections II, III, and IV.

As a result of considerations discussed in Section II, it turns out that air absorption is not properly modeled in our experimental situation. In full scale, atmospheric absorption is not a strong effect, but in our model, we are faced with sound attenuation of as much as 1 dB/ft. We must therefore subtract out this absorption if we are to simulate full scale conditions. Other factors that must be considered are effects of roughness on building faces and turbulence in the atmosphere. These are discussed in the sections that follow.

A major emphasis of this work is the correlation between the steady-state simulation experiments and the transient diagnostic studies. We require that the transient experiments be consistent with the steady-state experiments in terms of energy gain (loss) due to reflection (shielding) effects. In addition, of course, we require that the transient experiments also provide us with information on the actual paths being taken by the sound energy in travelling from the source to the microphone. This interpretation of the experimental work is contained in Section V of the report.

The propagation effects of streets and buildings that cause the sound levels to differ from what they would be in open, flat terrain are lumped together into a "Transmission Gain" (TG). A major part of the work presented here is the experimental evaluation of TG for various model configurations, flight paths, and microphone locations.

Finally, we believe that this work leads us naturally to a position where we are ready to expand the model to include a larger section of an urban area near a STOL or Verti-Port. In Section V, we describe some of the considerations pertinent to this extension of the work reported here. We also believe that we are now ready to make correlations between our

laboratory data and field experiments. The plans for such a correlation are also discussed in Section V.

## II. Scaling Laws and Modeling Techniques

### Dimensional Scaling

The fundamental scaling relationship in acoustics is the ratio of sound wavelength  $\lambda$  to geometric length  $L$ . Thus, if the sound speed in the medium remains unchanged, the constancy of the ratio  $L/\lambda$  requires that  $fL$  be constant also. In our work here, the length ratio is 1:32 so that the ratio of frequencies in the model to full scale must be 32:1.

The concept of dimensional scaling may be understood by reference to Fig. 1. In this figure, we show two situations in which the dimensional relationship of all objects is in a scale of 1:4. If the sound field in the two cases is to be similar (due to geometric effects only), then the wavelength of sound in the two cases must scale in exactly the same way that the building dimensions and the positions of source and receiver do.

In a mathematical sense, the basis of this relation arises from the fundamental acoustical equation, which is

$$(\nabla^2 + k^2)p = 0 \quad (1)$$

where  $\nabla^2 \equiv \frac{\partial^2}{\partial x^2} + \frac{\partial^2}{\partial y^2} + \frac{\partial^2}{\partial z^2}$ ,  $k = \frac{2\pi}{\lambda}$ , and  $p(x,y,z)$  is the pressure. If we non-dimensionalize this equation by forming new variables  $x' = x/L$ ,  $y' = y/L$ , and  $z' = z/L$ , where  $L$  is a typical length in the problem, the resulting equation is

$$\frac{\partial^2}{\partial x'^2} + \frac{\partial^2}{\partial y'^2} + \frac{\partial^2}{\partial z'^2} p(x',y',z') + (kL)^2 p(x',y',z') = 0 \quad (2)$$

Thus, if we keep  $kL = 2\pi L/\lambda$  constant as we change from one scale to another, the form of the wave field will remain unchanged, which is the goal of the modeling procedure.

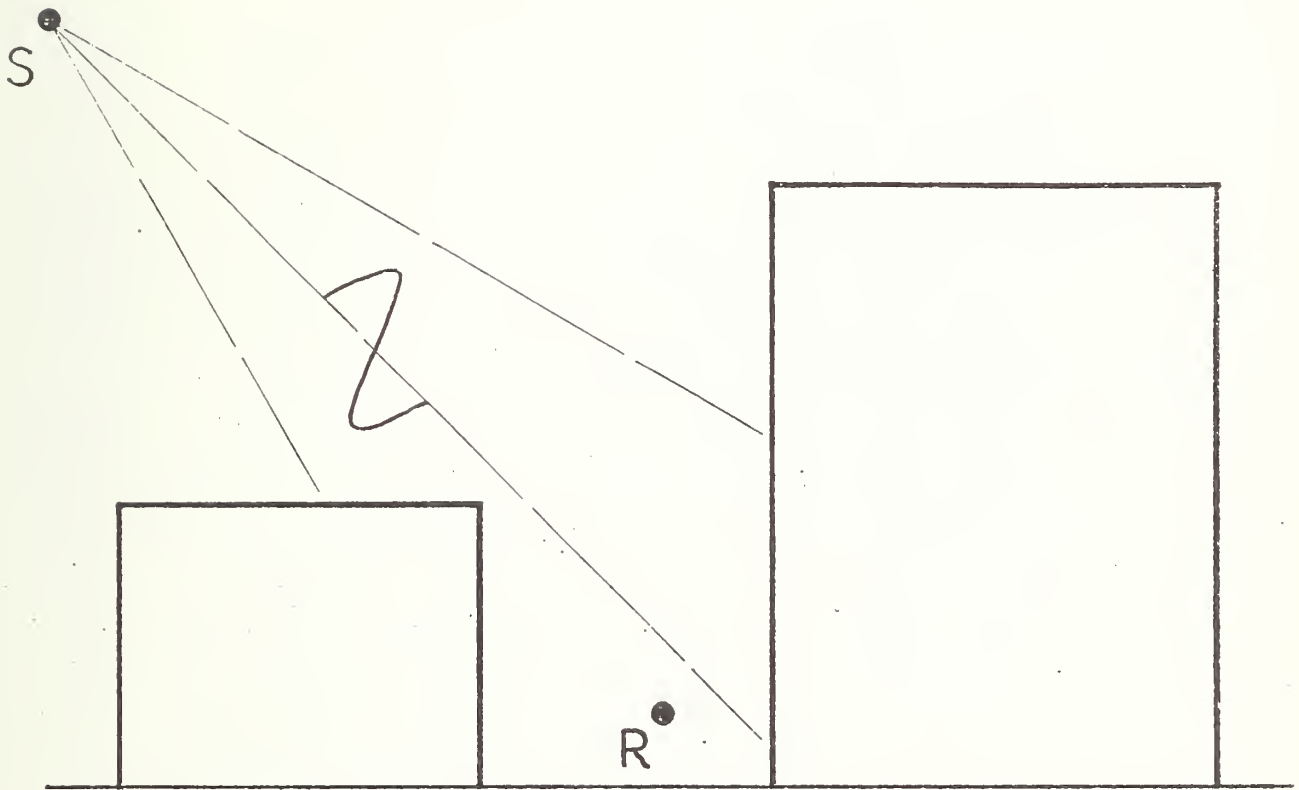
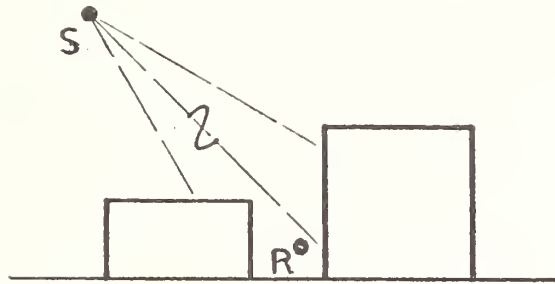


Fig. 1. Illustration of 4:1 scaling of dimensions and wavelength.

Strictly speaking, the dimensional scaling of a city street for geometric effects in acoustics requires that all geometric features be scaled. This would mean the preservation of such details as building facades, doorway insets, roof overhang, street profile, etc. Since it is not desirable to build more detail into a model than is necessary, one can examine the effect of such irregularities by adding diffusing or roughness elements to a smooth walled model. We have not done this at the present time in our model work, but such experiments are planned for future work.

### Modeling Absorption

The two principal forms of absorption for aircraft noise projected into city streets are those due to viscosity of the air and the losses upon reflection from the buildings, street surfaces, etc. Let us deal with the problem of reflection losses first, and then discuss air absorption.

Reflection losses in acoustics are expressed by an absorption coefficient  $\alpha$ , the fractional amount of sound energy extracted from the sound wave upon reflection. This coefficient can range from near unity for certain sound absorbing treatments to a few percent for surfaces such as tile, concrete, or glass. These latter materials are those used for the exteriors of buildings and therefore, unless there are many reflections of sound from these surfaces (as there are in a room), this absorption mechanism will not be of great significance. The "open top" nature of the street as an acoustical space generally precludes such a large number of reflections - in most of the data presented here, only 3 or 4 reflections are important at most.

In certain cases, when the sound propagates in directions that are nearly parallel to the ground, the effect of ground absorption (or finite

impedance) can be greatly enhanced. In such cases, some attempt at ground impedance simulation may be made, as has been done by Delaney<sup>1</sup> and Auzou<sup>2</sup>. Because of the relatively high angles of incidence in our experiments, simulation of the ground impedance is not considered by us to be necessary.

Air absorption due to viscosity arises from both shear and bulk viscosity effects. The shear viscosity  $\eta$  and the thermal conduction losses combine to produce the "classical" attenuation, which is given by

$$\begin{aligned} \mu_{\lambda}^C &= \frac{8}{3} \pi^2 \frac{\eta}{P_0} f \quad \text{nepers/wavelength} \\ &\doteq 2.3 \times 10^2 \frac{\eta}{P_0} f \quad \text{dB/wavelength,} \end{aligned} \quad (3)$$

where  $P_0$  is the pressure and  $f$  is the frequency. At relatively high frequencies (above 10 KHz) in fairly dry air (1% R.H. at 70°F), one can achieve this attenuation. For most cases, however, bulk viscosity effects due to the "relaxation" of vibrational degrees of freedom of the oxygen and and nitrogen in the air dominate the air absorption.

Fairly recent work by Evans and Sutherland<sup>3</sup> and by Piercy<sup>4</sup> appear to explain air absorption quite well and provide excellent guidance for modeling studies. In Fig. 2, we show the attenuation per wavelength plotted by Piercy for a humidity of 37% at 70°F. In the range from 500 Hz to 4000 Hz (the dominant bands in aircraft noise and urban noise) the attenuation is about  $2 \times 10^{-4}$  nepers/wavelength, whereas the attenuation at 32 KHz (a frequency used in our modeling work) the attenuation per wavelength is about  $10^{-3}$  nepers/wavelength. In the work reported here, we have not scaled the air absorption, but instead we have subtracted the air absorption out of the data, as discussed in Section III.

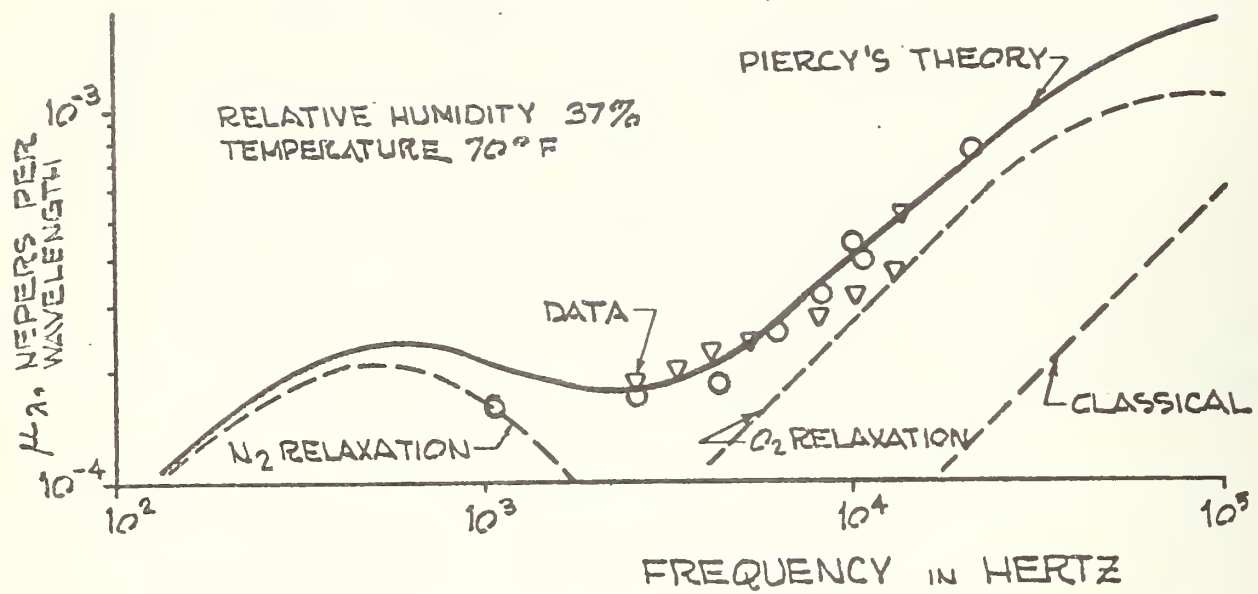


Fig. 2. Air absorption under normal laboratory conditions.

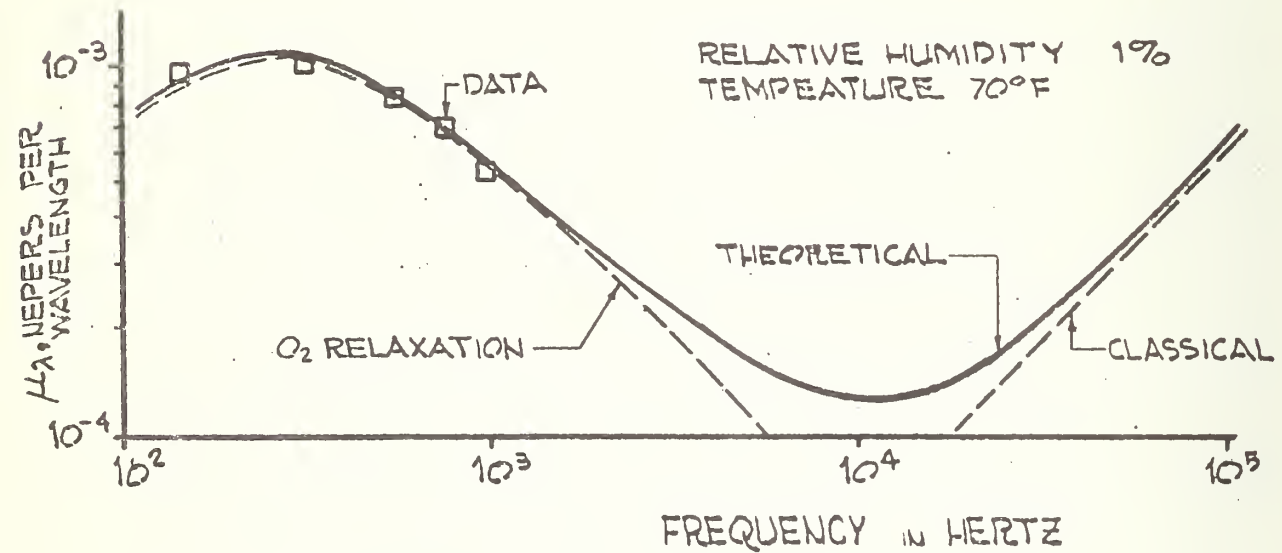


Fig. 3. Air absorption using dried air in laboratory.

Piercy's calculation for air absorption at 1% R.H. at 70°F is shown in Fig. 3. At 20 KHz and above, the attenuation is set by the classical attenuation given in Eq. (3). We see that at 32 KHz the attenuation in nepers per wavelength is about  $2 \times 10^{-4}$ . Thus, by drying the air sufficiently, we could eliminate the necessity for mathematically correcting our data for air absorption and simulate the full scale situation directly. We plan to do this in future efforts.

#### Scaling and Selection of Source Parameters

A full simulation of an aircraft noise source would reproduce the time pattern of sound pressure radiated in various directions from the source, with frequencies suitably scaled as mentioned previously. Such a simulation is possible in part by recording the noise of the aircraft, speeding up the replay by the scaling factor, and driving a small sound source. There are severe frequency response and power limitations in such an approach however, and we have chosen to simulate the band power levels of the noise source instead of the detailed time history. We note however that such a simulation might be quite useful, particularly for some of the lower frequency rotational noise components of a helicopter.

The octave band pressure level  $L_p^{OB}$  (dB re .0002  $\mu$ b) due to a source in air of power level  $L_\pi^{OB}$  (dB re  $10^{-12}$  watt) and directivity index DI is given by

$$L_p^{OB} = L_\pi^{OB} + DI - A_g - A_a + TG - 10 \quad (4)$$

where  $A_g = 20 \log r/r_o$  ( $r$  is the distance from the source in meters,  $r_o$  is a reference distance),  $A_a = 8.7 N\mu$  is the air attenuation where  $N$  is the number of wavelengths from the source to receiver ( $\mu$  is in nepers/wavelength),

and TG is the transmission gain representing the effects of buildings, streets, etc. Clearly, the simulating source should have a known power level and directivity index.

The source we have used for simulation is shown in Fig. 4. It consists of 4 small jets that are operated at 40 psi gage pressure. These jets impinge on each other and produce a broad band noise source that has uniform DI in the plane P shown in Fig. 4. Such a source has been described previously by Veneklasen.<sup>5</sup> Instead of using the power level to specify the source, we have used the octave band sound pressure level at a reference distance  $r_o$ ;  $L_o^{OB}$ ,

$$L_p^{OB} = L_o^{OB} - A_g - A_a + TG \quad (4')$$

The values of  $L_o$  in bands at  $r_o = 1$  ft are shown in Fig. 5. The DI of this source for directions along the axis A in Fig. 4 is about 4 dB higher than in the plane P. In experiments described in Section III, we attempted to keep the source oriented so that the levels in Fig. 5 represent the effective source strength.

In the "diagnostic" experiments, we want to determine the paths that the sound takes in traveling from the source to the microphone. For these experiments, we need a source that generates a short, highly reproducible sound pulse with appreciable sound energy in the octave bands from 16 to 128 KHz. A spark source that meets these requirements has been developed for this project and is shown in Fig. 6. The spectrum of the peak sound pressure when electronically processed as described below is shown in Fig. 7. The waveforms of the sound pulse produced when passed through a third octave filter is shown as an inset in Fig. 7. The duration of the pulse is short enough so that differences in path lengths of a few inches may be resolved

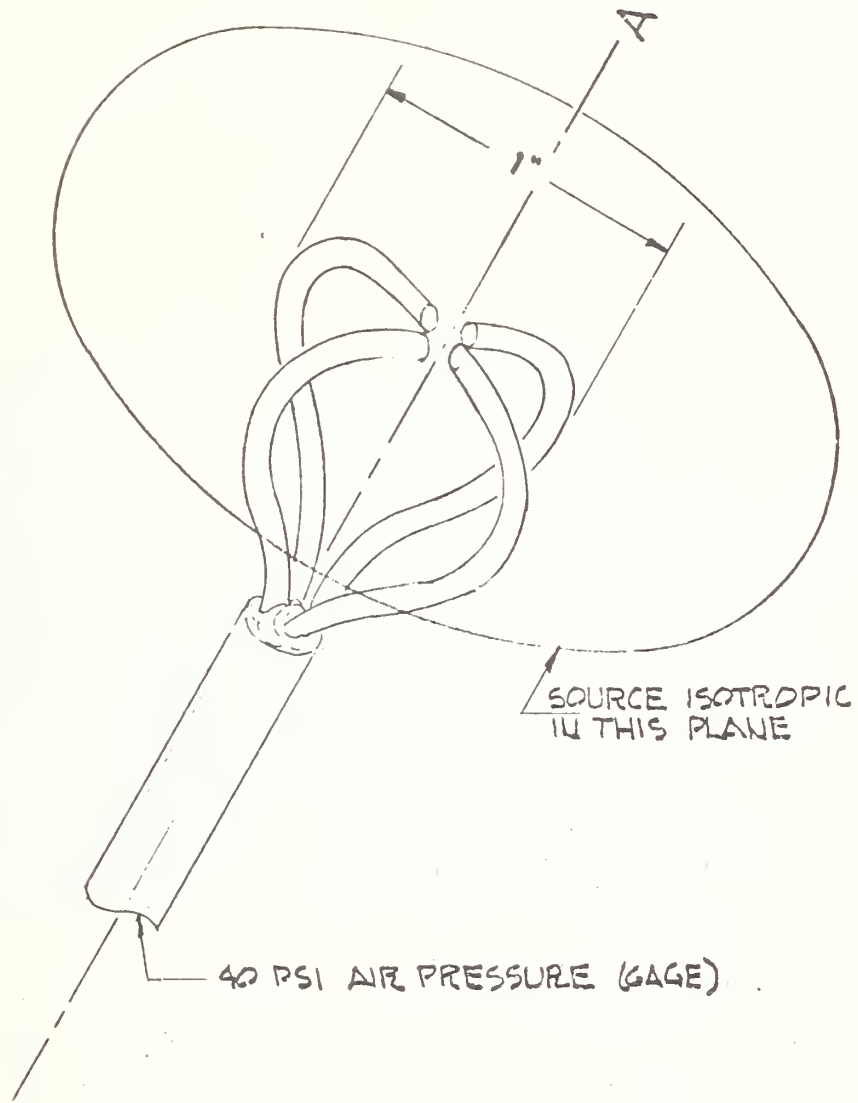


Fig. 4. Steady-state broad band noise source.

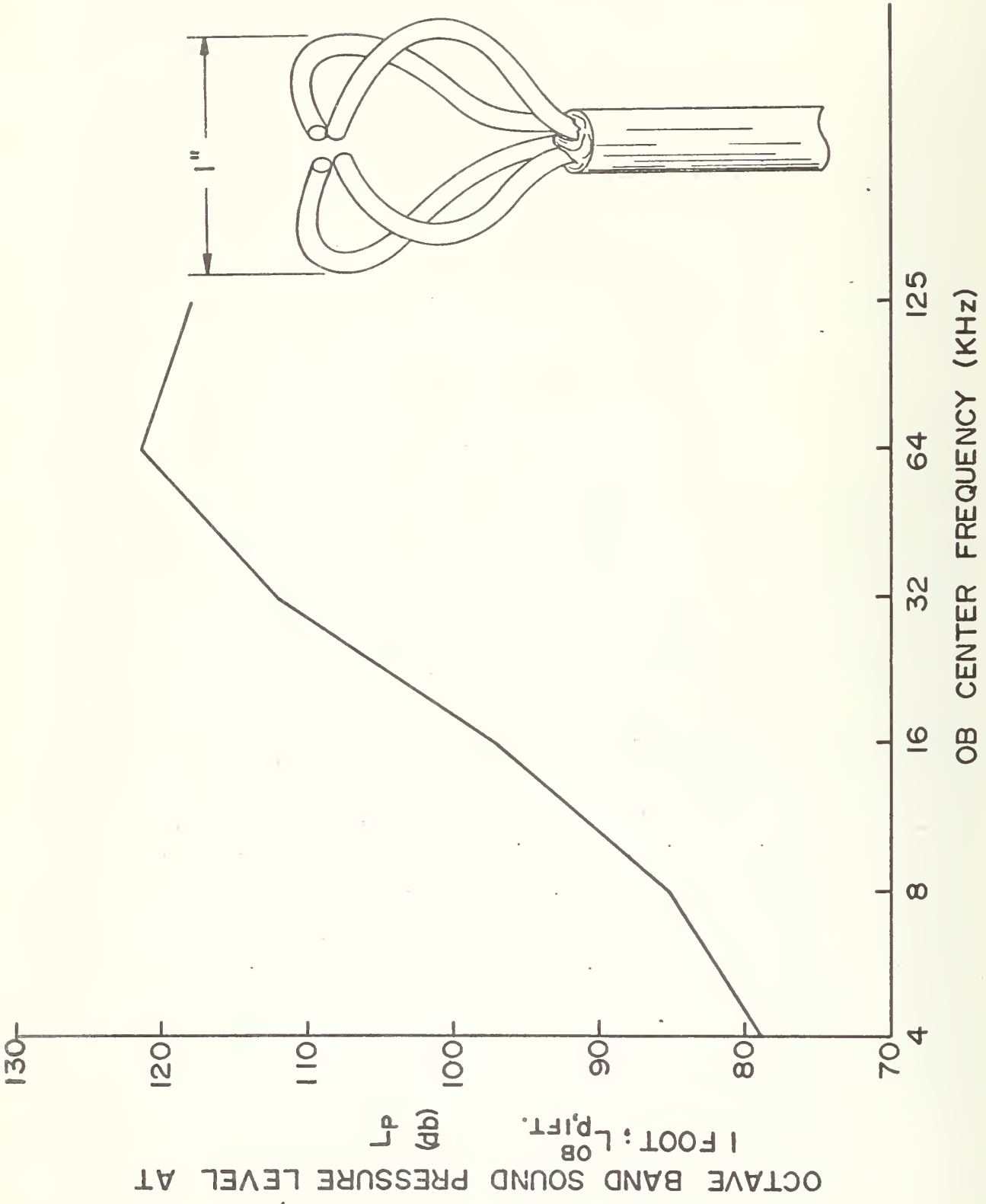


Fig. 5. Spectrum of steady-state noise source, measured at 1 foot.

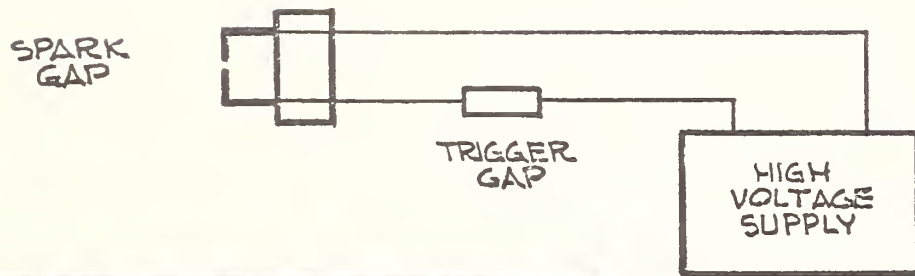


Fig. 6. Spark gap transient sound source.

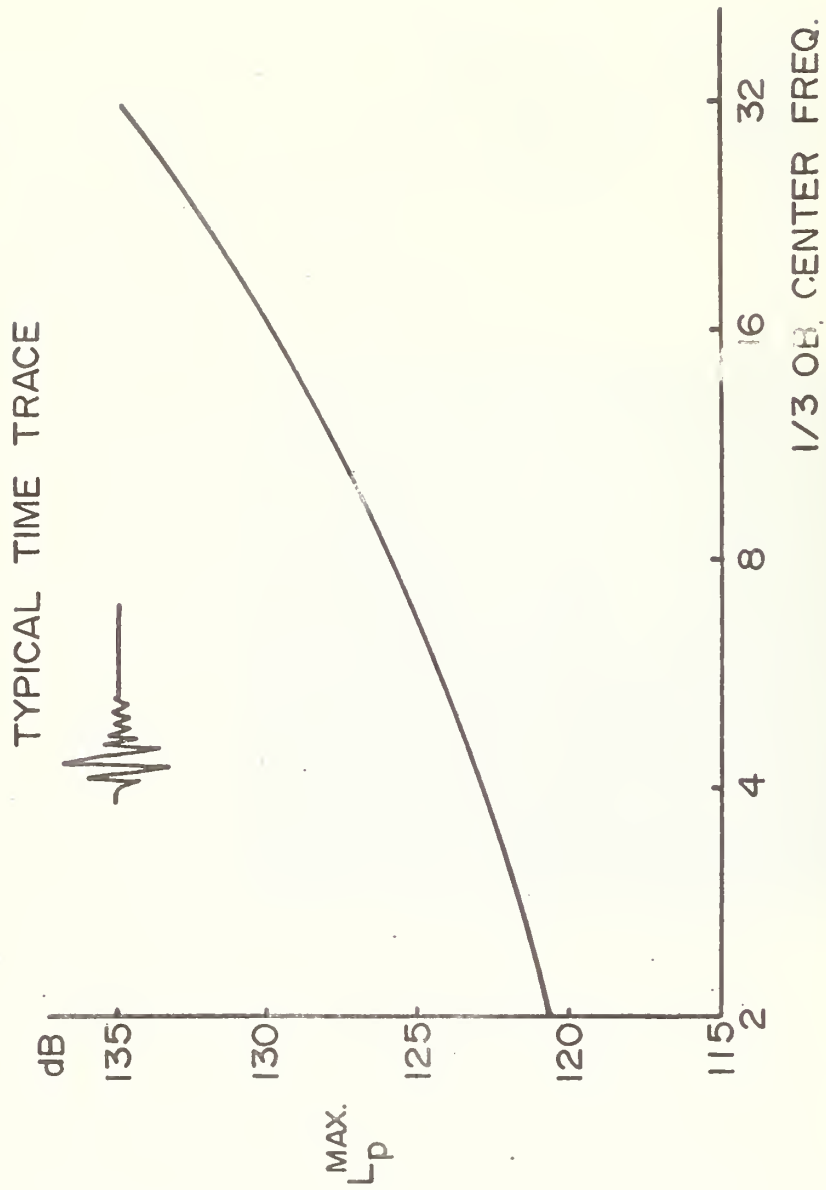


Fig. 7. Energy spectrum of spark source in 1/3 octave bands.

from the pulse train arriving at the microphone.

### Instrumentation

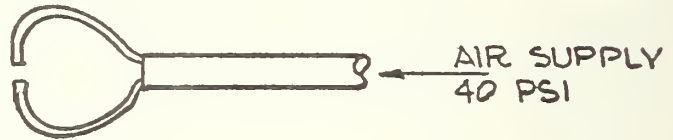
The instrumentation line-up for steady state noise measurements shown in Fig. 8 is relatively straightforward. The principal difficulties lie in microphone selection. We chose a BBN 0.1 inch crystal microphone because of its small size and high resonance frequency (in excess of 100 KHz). The disadvantages with the microphone are its low sensitivity and high noise floor, which require that the sound source be relatively intense.

The filter set is the B&K model 1614, which has 1/3 octave filters up to 160 KHz. The sound level in each band is measured with a B&K model 2607 Measuring Amplifier.

The instrumentation for impulse measurements is more complicated than for steady measurements. The equipment line-up for this case is shown in Fig. 9. The third octave band filter is used to form the pulse shown in Fig. 6. The measuring amplifier has been specially modified so that very short averaging times (order of 0.5 msec) may be used for the log rms output. This output is then fed to a Biomation model 802 transient recorder. Graphical output is recorded from a cathode ray oscilloscope. Several examples of records obtained from this set-up are shown in Section IV.

# STEADY STATE NOISE EXPERIMENT

## SOURCE



## SENSOR

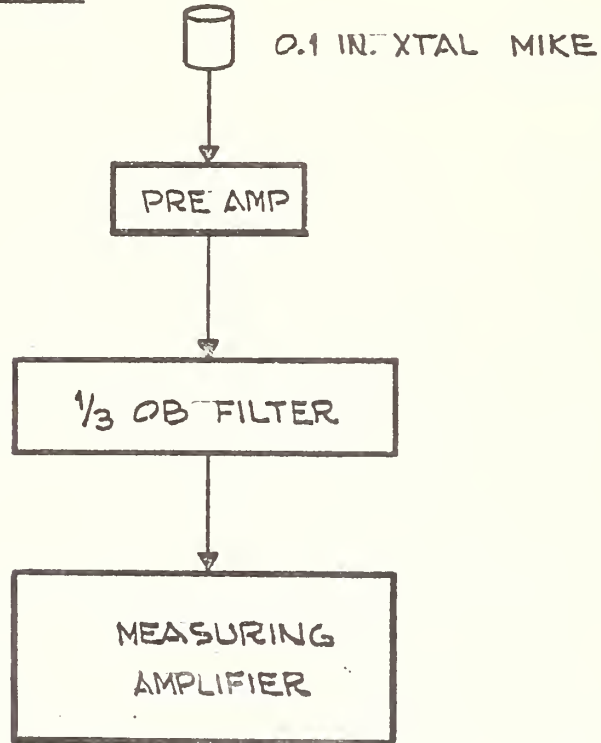


Fig. 8. Line-up of steady-state instrumentation.

# TRANSIENT NOISE EXPERIMENT

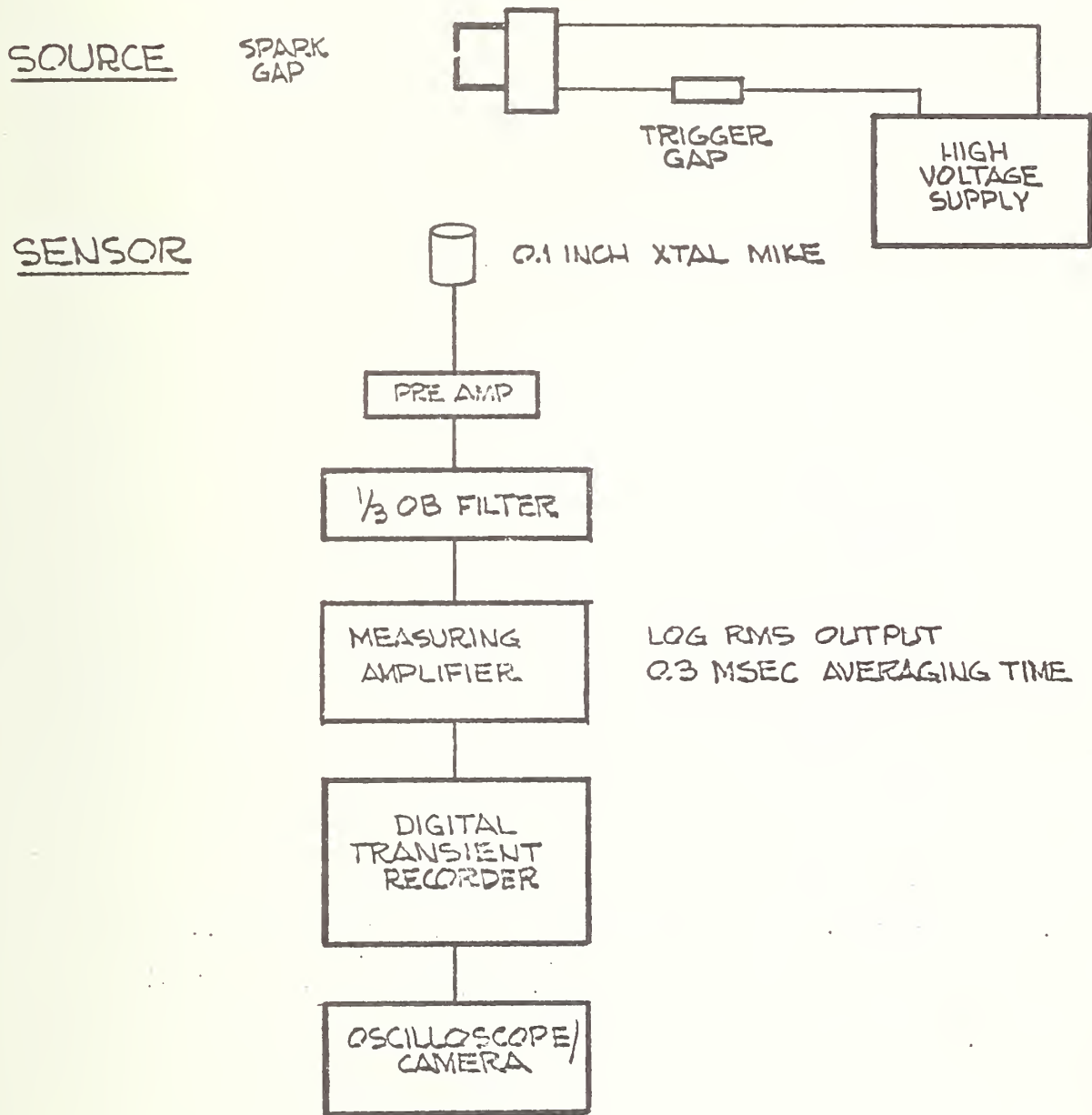


Fig. 9. Equipment line-up for transient experiments.

### III. Steady-State Experiments

As we discussed in Section II, the aim of these experiments is to simulate the flyovers of an aircraft over a particular feature of urban terrain and to find the spatial distribution of the sound at street level. Estimates of noise levels in an urban situation can be compared with open terrain noise predictions. This a particularly interesting aspect of modeling.

The steady state noise source described in Section II is used in the simulation of the flyover. The analysis of noise levels in the model is carried out for each octave band of interest. The experiments consist of traversing the noise source over the model and measuring the sound pressure level in each octave band for an observer at street level as a function of source position. The instrumentation used in processing the steady-state signals is shown in Fig. 8.

Simulating a flyover in a model experiment allows much more control over the experiment than one has in a field situation. We are able to choose a particular geometrical layout of streets and buildings along with the position of the microphone. Moreover, we can move the source at a constant desired height, and can hold it stationary at one position if necessary.

The two particular street configurations that we have studied are a "linear" street and an "L-shaped" street. The heights of the buildings on either side of the street are different. The layout is shown in Fig. 10. The source can be moved either across or along a street. The position of the microphone and the source path are shown in the figures for each set of experiments.

To get meaningful results and to present them in a form enabling us to

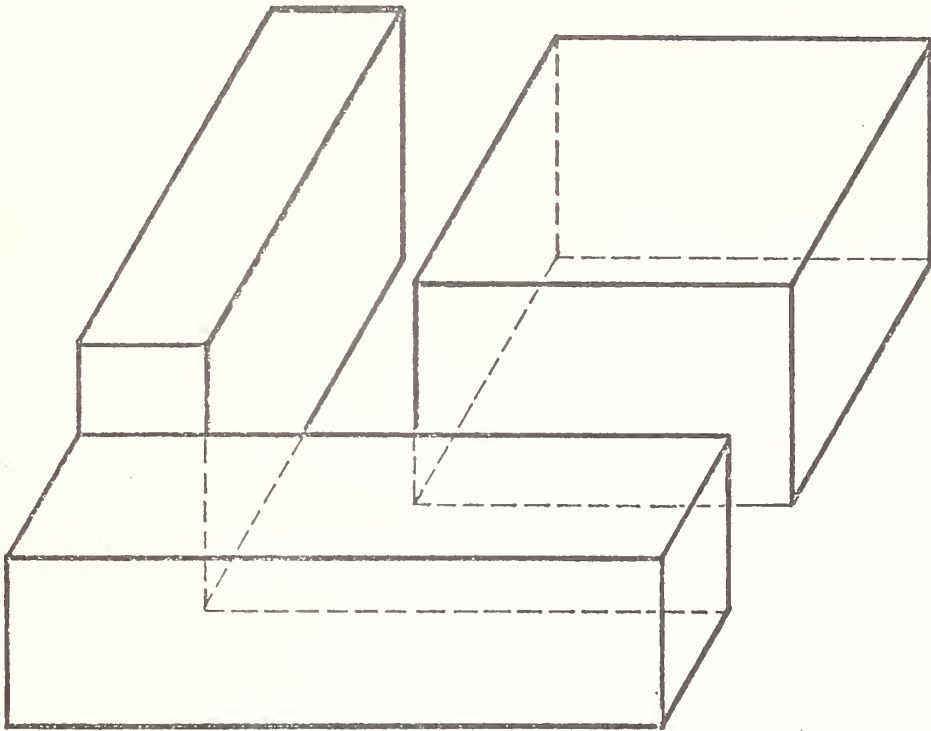


Fig. 10. Model configuration for street overflight experiments.

compare with open terrain conditions the procedure adopted was as follows. The experimental results provide us with the sound pressure level received at the microphone for a particular source position. These levels are recorded in the different octave bands having center frequencies from 4 to 128 KHz corresponding to the full-scale frequencies 125 Hz to 4 KHz. From this data we wish to obtain the transmission gain TG due to the geometry as defined by Eq. (4'). Solving this equation for TG results in

$$TG = L_p - L_p(1 \text{ ft}) + A_g + A_a \quad (4'')$$

where the quantities are as defined in Section II. The calculation of TG is carried out for each octave band and combination of source receiver positions.

The spectra and levels for a helicopter flyover over open terrain are also calculated. These are based on data for helicopter vortex noise assuming isotropic radiation<sup>6</sup>. The equation for the overall sound pressure at 30 ft from the helicopter is taken from Ref. 6:

$$L_p^{30'} = 10 \log [6.1 A_b V_{0.7}^6] + 20 \log C_L + 126 \text{ (dB)}$$

where we have taken the blade area  $A_b = 72 \text{ ft}^2$ , the blade speed at the 70% span position to be  $V_{0.7} = 500 \text{ ft/sec}$ , and the blade lift coefficient to be  $C_L = 0.4$ . Since our scaling is 1:32, this corresponds to our band pressure levels at a distance of 1 ft. From the spectrum of vortex noise given in Ref. 6, the sound pressure level in each full scale band relative to this overall level is as follows.

frequency (Hz)	500	1000	2000	4000
level relative to overall (dB)	-4	-7	-9	-13

Geometric spreading is taken into account to predict levels at the microphone location assuming open terrain propagation. Atmospheric attenuation at audible frequencies for the distances involved here may be neglected.

The values of Transmission Gain (TG) are now superimposed on these levels for each octave band (with the data for the 32 KHz octave band in the model corresponding to the full scale 1 KHz octave band) and corresponding positions. Figure 11 illustrates how this is done. The solid lines show the open terrain values obtained from the helicopter noise spectrum. Superimposed on them is the TG value obtained in the model for each position.

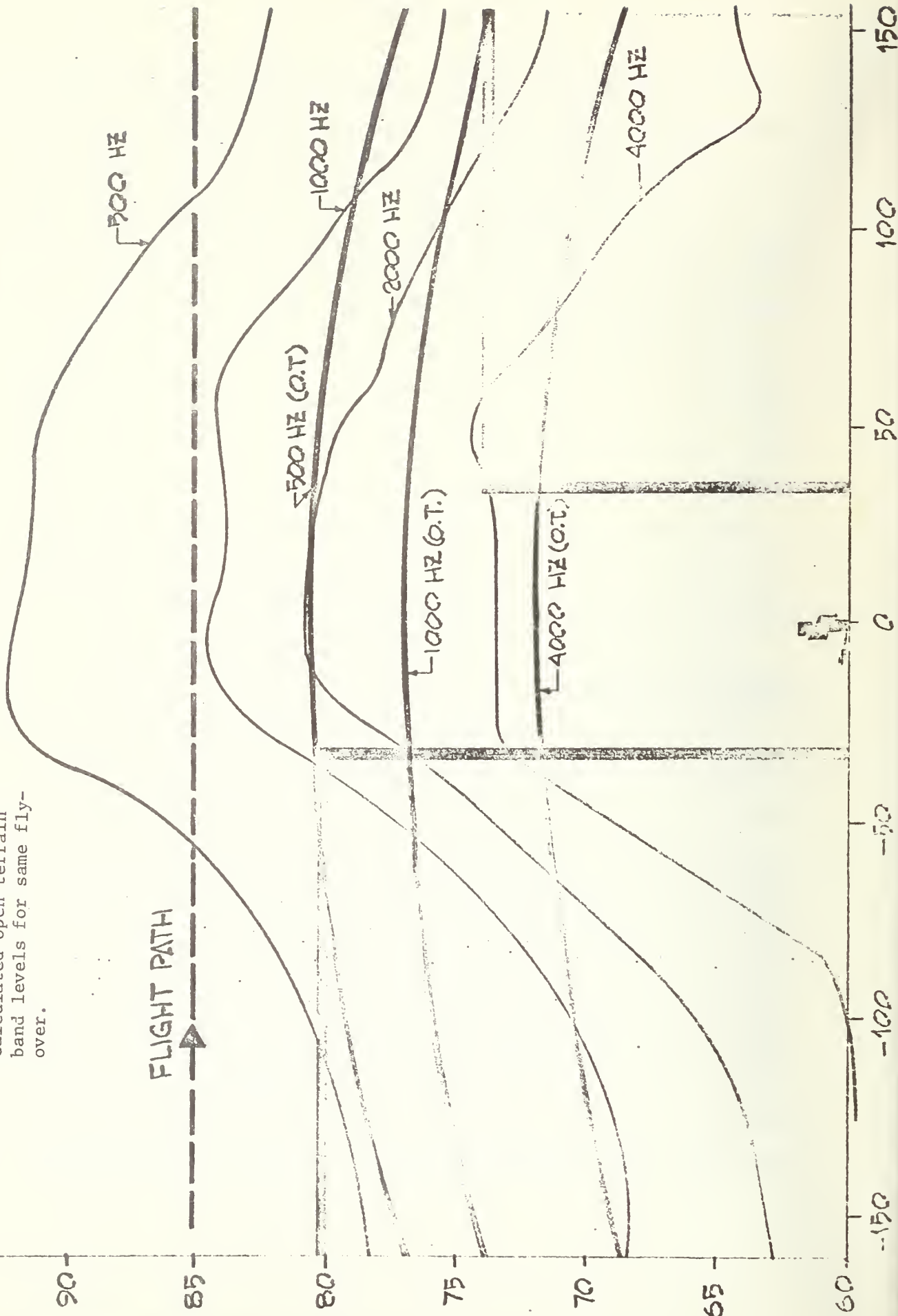
Using these octave band levels, we have computed the perceived noise level ( $L_{PN}$ ) for open terrain and for flyover across a street. The procedure for computing  $L_{PN}$  is that described in Ref. 7.

### Discussion of Results

We have used model transmission data to develop estimates of perceived noise level as a function of source position for several situations. The results are presented in Figs. 12 - 16. The model geometry is indicated on each figure, as are the positions of the source and microphone. The first question that arises is whether there are general differences between the "urban" noise levels and those computed for open terrain. To this end, we find from Fig. 12 that there are conditions of amplification of the noise when the levels are higher than those to be expected for an open terrain, and also there can be shielding effects when the levels are lower. We also note from Fig. 13, that the shielding and amplification effects are markedly reduced as the aircraft flies at even slightly higher altitudes

PNL = 100 dB

Fig. 11. Measured band levels and calculated open terrain band levels for same fly-over.



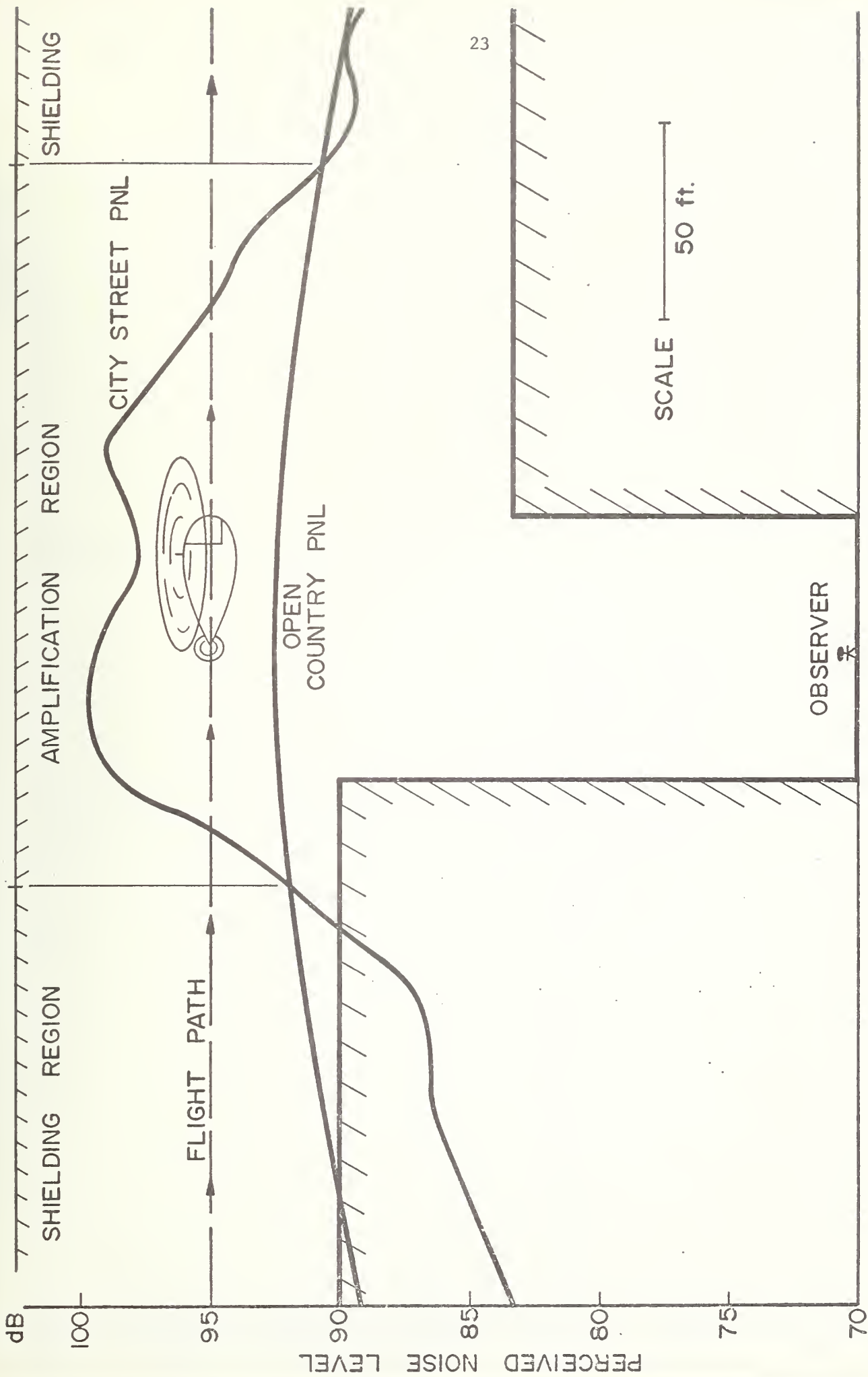


Fig. 12. The variation of Perceived Noise Level as a function of source position for flyover across a city street.

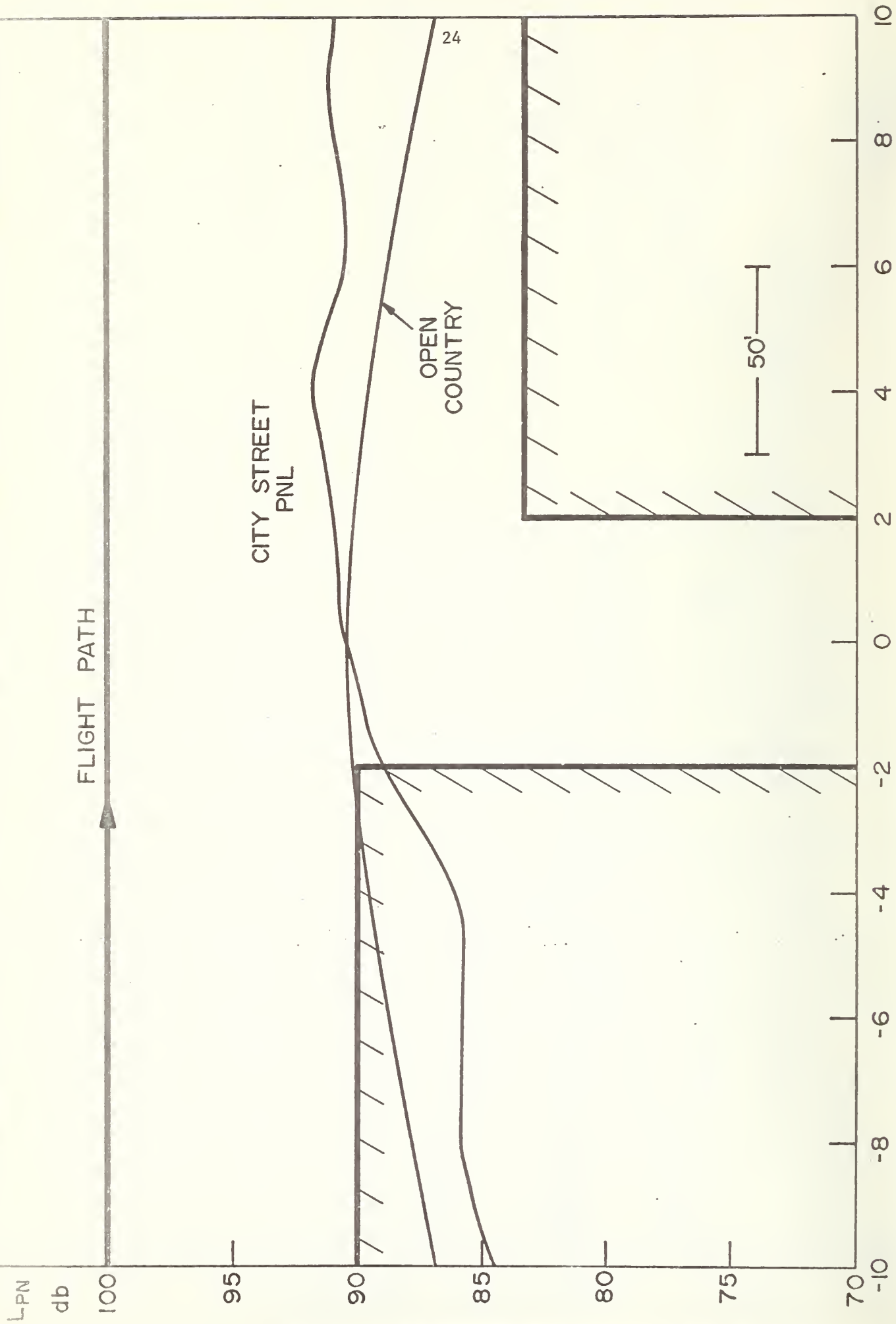


Fig. 13. The variation of Perceived Noise Level as a function of source position for flyover across a city street.

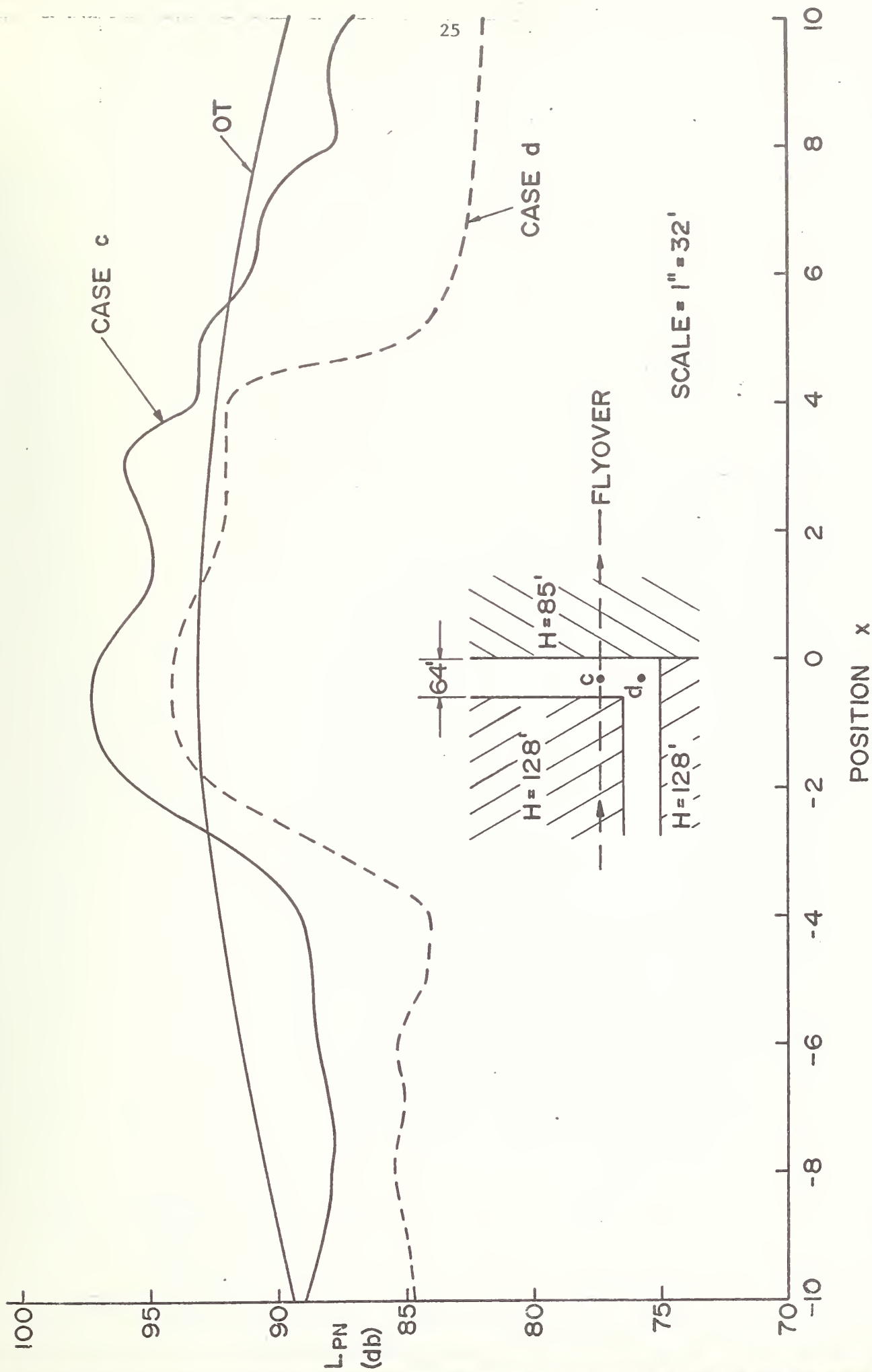


Fig. 14. Perceived Noise Level as a function of source position.

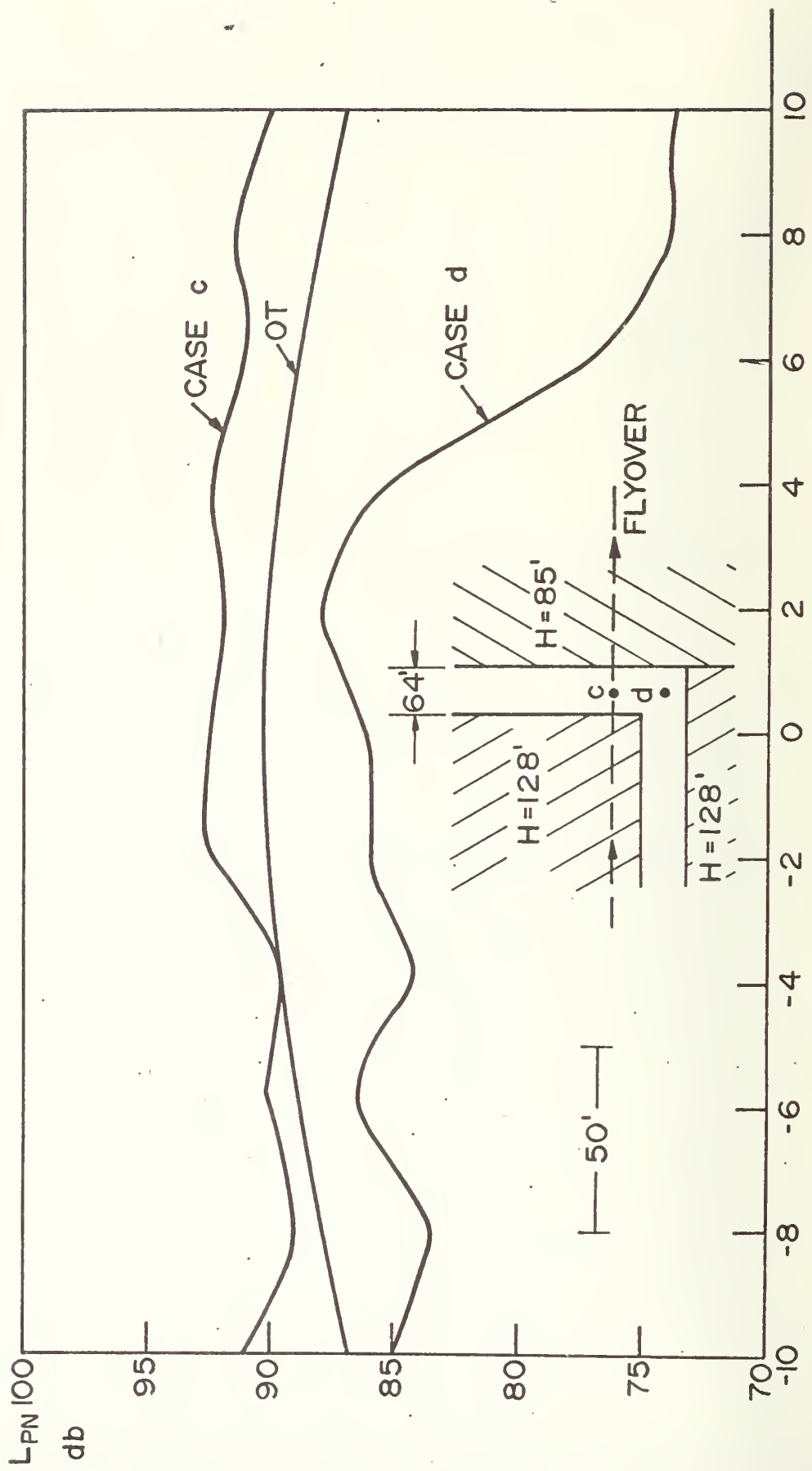


Fig. 15. Perceived Noise Level as a function of source position for flyover of L-shaped street.

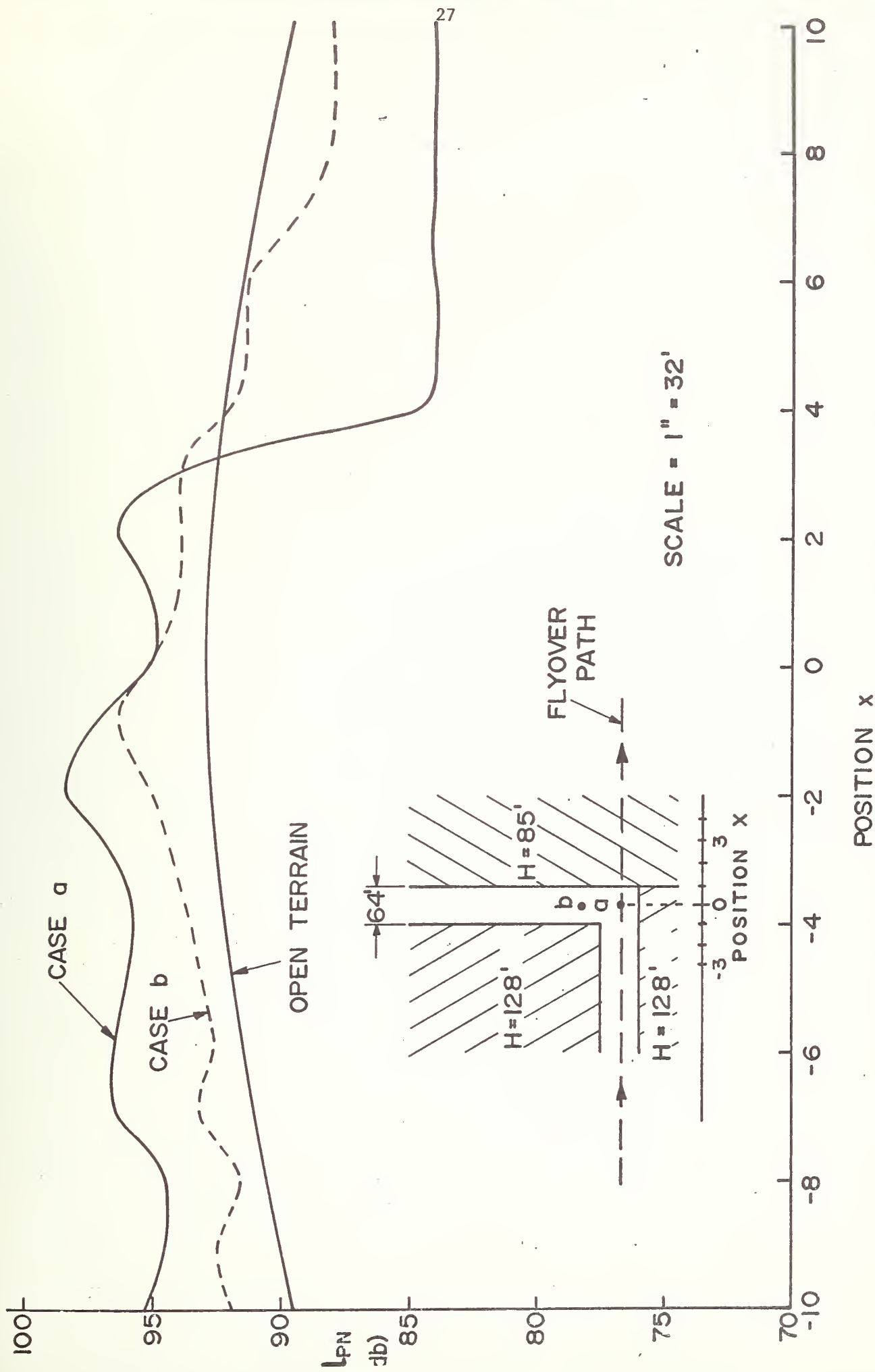


Fig. 16. Perceived Noise Level as a function of source position for a longitudinal flyover.

over the street.

The existence of side streets parallel to the flight path can diminish the shielding effect. If we compare the data in Fig. 12 to that of Case C in Fig. 14, we see that the shielding in positions -10 to -4 is less, and that the amplification at positions -2 to +2 is also less. Sound levels in Case C do not vary greatly from the open terrain values because of the reverberant build-up within the side street, and because the parallel street provides an alternate path for the sound to get to the receiver.

The position of the observer relative to the ground track of the flight path, i.e., whether he is directly below the flight path or displaced from it, emphasizes the effect of a corner. Referring to Figs. 14 and 15, we see that the levels are generally lower if the observer is not directly below the flight path.

Considering first the case of a linear street in Fig. 10 we observe that the shielding effect is important when the source is not in direct line of sight of the observer. The shielding effect of the higher buildings is about 7 - 8 dB. The shielding effect of the lower buildings is diminished due to the presence of higher buildings across the street which provide a reflecting plane and hence increase the sound levels at the observation point.

Referring to Fig. 12 and Fig. 13 we observe that as the altitude of the flyover increases, the overall levels decrease, but also the shielding effect of buildings becomes less.

Figures 12 and 16 show the effect of a longitudinal flyover along a street and transverse to a street. The data indicate the channelling effect of a side-street: causing the levels to remain fairly uniform (Case A, B in

Fig. 16) until the source is above the buildings.

We see that the simulation of a flyover in the model can reveal interesting features of the sound propagation process. The data indicate that the steady-state noise source can be used to investigate the shielding and amplification effects of the buildings on the distribution of sound, as well as provide a way of predicting noise impact due to a flyover. In the following section, we examine the propagation paths more closely with the diagnostic aid of transient experiments.

#### IV. Transient Experiments

Although V/STOL aircraft generate transient sounds such as the blade slap due to rotor-vortex interaction, our interest in transient experiments is not in simulation. Rather, we use transient studies in a diagnostic way - to determine the various paths that the sound energy takes in traveling from the source to the receiver, and the relative amount of sound power contributed by each path to the overall sound level. We shall discuss how these needs are met in the following.

The instrumentation line-up used in the processing and recording of transient data is shown in Fig. 9. The equipment consists of a measuring amplifier and octave filter set, transient recorder and an oscilloscope with camera. In the transient experiments, the log rms of the 1/3 octave filtered pressure signal from the microphone is displayed and photographed from the oscilloscope face. In most cases, only the first 20 milliseconds of this signal have been recorded since this period includes the most prominent paths of propagation in terms of energy content.

In order to determine the absolute sound pressure level of the different parts of the transient signal, the instrumentation chain was calibrated. The horizontal line on each photograph marks the 124 dB sound signal generated by the B&K Pistonphone. In most cases, the oscilloscope was adjusted so that one vertical centimeter on the face represented 10 dB, see for example, Fig. 17.

As seen in the photographs in Figs. 17 and 19, most signals consist of one or more pulses arriving in a series. By reading the time of arrival of a given pulse from the photograph, it was possible to determine the total length of the path of propagation for that pulse. By comparing this path

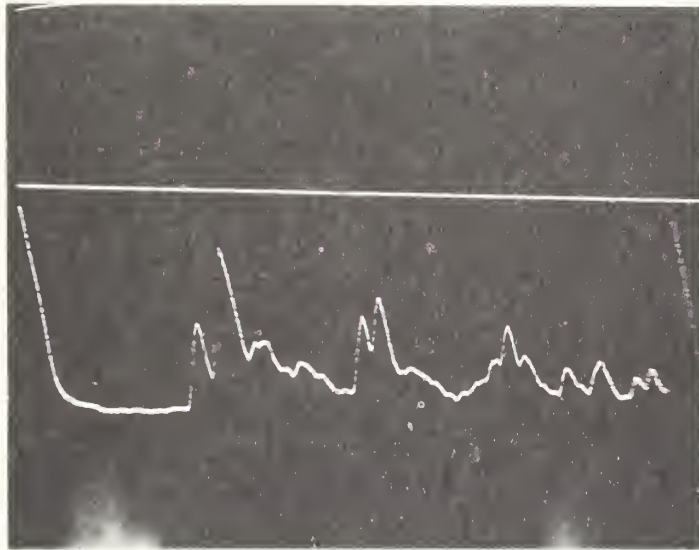


Fig. 17. Time pattern for sound pressure for position B. [32 KHz octave band] (Horizontal line marks 124 dB).

length to the lengths of different possible paths as measured on a scale drawing of the street models, it was possible to develop a correspondence between paths of propagation and the transient pulses.

As one example, consider the photograph for position B (32 KHz octave band) in the linear street model shown in Fig. 18. Two primary pulses are shown in the photographs of Fig. 17; one that arrived after 5.8 milliseconds and another after 6.2 milliseconds. The pulse that arrived after 5.8 milliseconds must have traveled approximately 6.5 feet, taking the speed of sound in air to be 1127 ft/sec.

The measured length of the diffracted path from position B to the microphone is approximately 6.4 feet (see Fig. 18). Thus, it was concluded that the first pulse shown in the photograph resulted from the diffraction of the transient signal off of the taller building.

Likewise, the second pulse shown must have traveled approximately 7.0 ft. As measured from a scale drawing, the length of the first reflected path from position B to the microphone is approximately 7.1 ft. Thus, it may be concluded that the second pulse shown in the photograph must have resulted from a single sound reflection off of the smaller building.

As another example, consider the photograph for position F (32 KHz) in the linear street model as shown in Fig. 19. The earliest major pulse shown has arrived after 5.0 milliseconds which means it must have traveled approximately 5.6 feet. From a scale drawing of the linear street model, the length of the direct path from position F to the microphone is 6.3 ft (see Fig. 18). Thus it may be concluded that the first pulse arrived via the direct path. In the same manner, it was concluded that the second pulse shown in the photograph for position F arrived via a path that

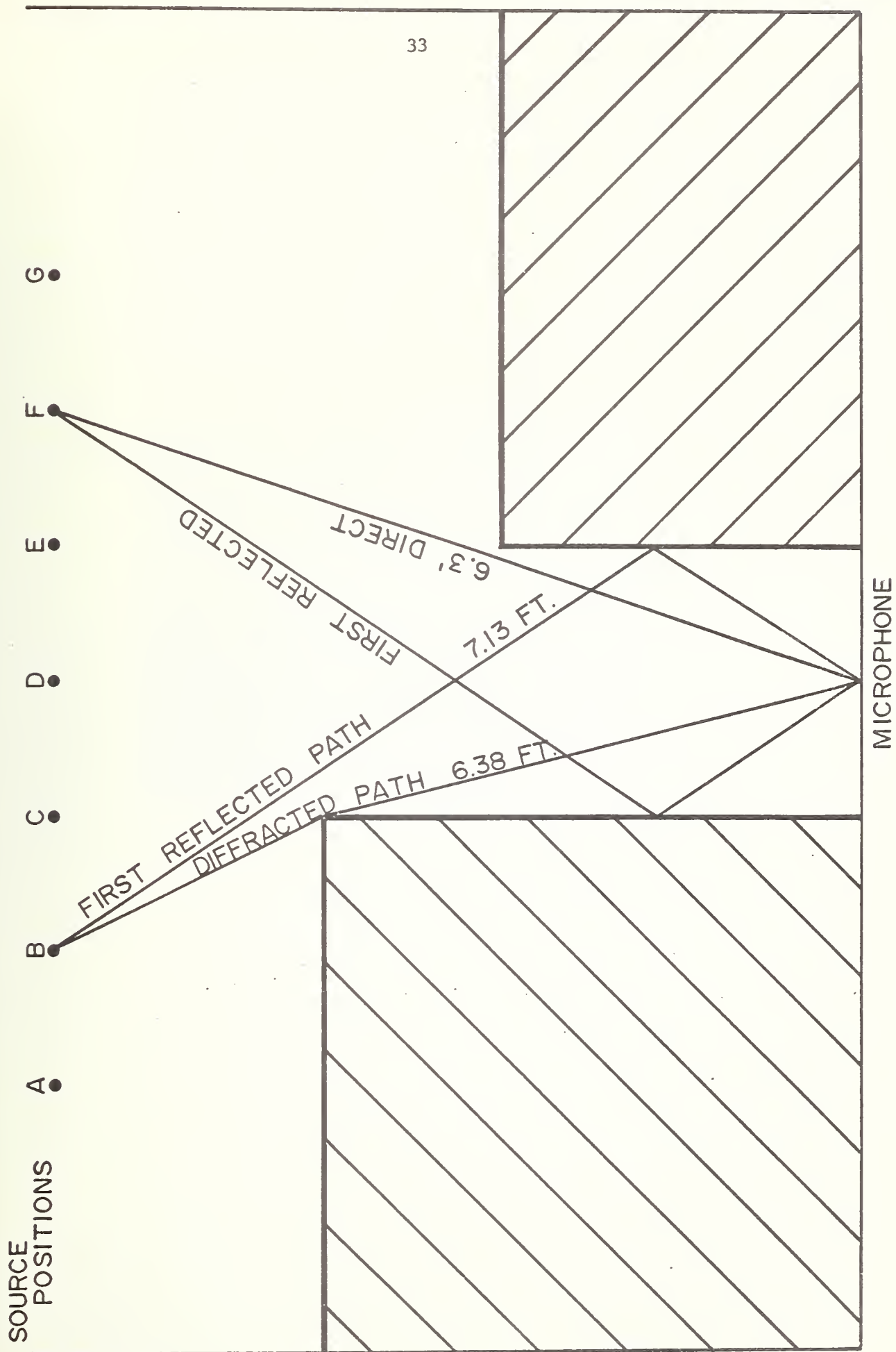


Fig. 18. Cross-section of model city block - scale: 1" = 1'.

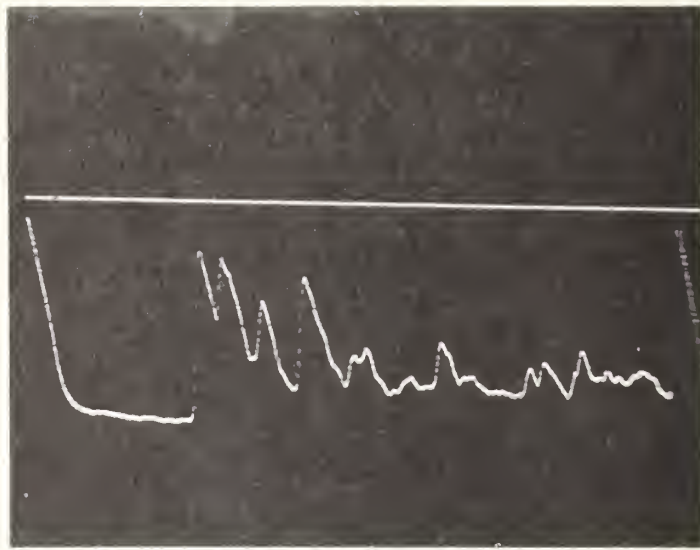


Fig. 19. Time pattern of sound pressure  
for position F. [32 KHz]

reflected once off of the taller buildings (compare Figs. 17, 19).

With the simple analysis described here, it was possible to interpret, for a given source position, a transient signal in terms of the paths of propagation that make it up. In this way, those paths of propagation which contributed most to the acoustical energy incident on the microphone could be determined.

The photographs taken for the different source positions and street configuration are useful in indicating reverberant build-up and the channel-like propagation of sound. To illustrate, consider the photographs for positions A and F in the L-shaped street configuration as shown in Figs. 20 and 21 respectively. The photograph for position A clearly indicates that a reverberant build-up lasts for about 4 milliseconds (128 msec full scale) while for position F, a reverberant build-up is not so apparent. This difference in reverberation is understandable as position A allows for channel-like propagation down the L-shaped street while position F does not involve such a large number of reflections in establishing the sound level at the microphone.

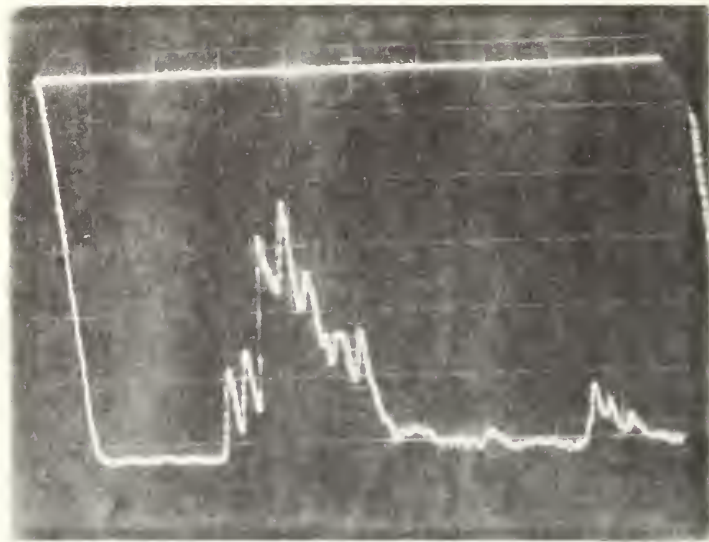


Fig. 20. Time pattern of sound pressure  
for position B. [32 KHz]

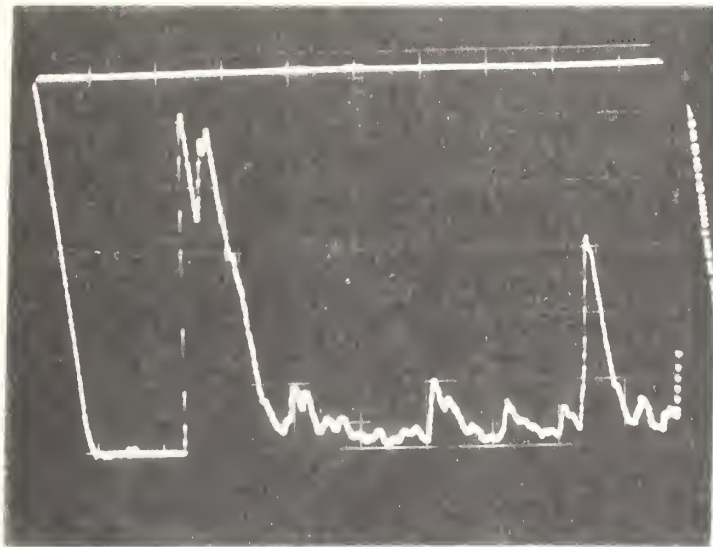


Fig. 21. Time pattern of sound pressure  
for position F. [32 KHz]

## V. Discussion and Summary

### Correlation of Steady-State and Transient Experiments

We can see intuitively that the energy of the sound pulses arriving at a microphone may add up to a total energy in the transient signal that is greater than that which would be present in the absence of reflecting (and shielding) surfaces. Thus, if a reflecting surface produces a second, equally energetic pulse to the signal arriving directly at the receiver from the source, the energy in the received signal is increased by 3 dB. This suggests that for steady-state noise sources, a similar result will hold, i.e., the level of the m.s. pressure at the microphone is increased by 3 dB when a second path is available of equal strength to the direct one.

The formal derivation of this equivalence between steady-state noise and transient pulses is well understood,<sup>8</sup> and we shall merely use the result in our work. The meaning of the result is that we can use the temporal structure of the pulse train at the receiver to determine the paths of propagation and use their amplitudes to determine the relative contributions of each path to the m.s. pressure at the receiver for a steady noise source like that described in Section III.

### Comparison of Steady-State and Impulse Data

Let us now compare the steady-state results to the transient results for a given source position and street configuration. The energies of the prominent peaks (obtained from the transient data) are first summed. This summation gives us an overall equivalent sound pressure level for a single pulse at a distance of one foot from the source. By directly measuring the maximum pressure level of the source at one foot, we can assess the effect

of the presence of buildings on the energy of the transient signal. As mentioned above, this energy comparison allows us to compare the steady-state and transient results.

In order to perform the energy summation, it was necessary to eliminate the losses due to air absorption and geometric attenuation from the pulse data. For example, the summation of data taken at position A in the L-shaped street (see Fig. 20) configuration is given in Table 1.

The peak sound pressure level of the transient source was measured at a distance of one foot. The peak level was found to be 134 dB as indicated in Fig. 22. Graphs of the summed one-foot levels versus source position for both street configurations are given in Fig. 23. The dotted horizontal line in these graphs represent the 134 dB comparison line. The difference between these curves and the 134 dB line is the Transmission Gain as determined from the transient data.

A comparison of the Transmission Gain as determined from the transient and steady-state data is shown in Fig. 24. We see that there is general agreement in the values of TG as determined by these two procedures, but we hope that in our future work we can improve the correlation between these procedures.

#### Effective Travel Distances

The transient data provides information as to the "effective" travel distance from source to receiver. This is the distance that most of the sound energy must travel. It will, in general, not be equal to the straight line distance between the source and microphone. This distance which is determined from the transient data can then be used in further computation of geometric and air attenuation.

TABLE I

Summation procedure as used on the photograph for position A in the L-shaped street configuration (see Fig. 20). The three highest peaks were chosen.

1. From the photograph:
 

a) $L_P$ of each peak: <ol style="list-style-type: none"> <li>i) 110 dB</li> <li>ii) 113 dB</li> <li>iii) 107.4 dB respectively.</li> </ol>	b) Times of arrival (t): <ol style="list-style-type: none"> <li>i) 7.0 milliseconds</li> <li>ii) 7.8 milliseconds</li> <li>iii) 8.5 milliseconds respectively.</li> </ol>
---	---
  
2. Knowing the times of arrival, the length of the paths of propagation for each peak were calculated:  $d = t \times 10^{-3} \times 1127 \text{ ft/sec}$ 
  - i) 7.9 ft
  - ii) 8.8 ft
  - iii) 9.6 ft respectively.
  
3. These path lengths were then multiplied by the absorption factor for air:  $A = d \times 0.3 \text{ dB/ft}$ 
  - i) 2.07 dB
  - ii) 2.34 dB
  - iii) 2.58 dB respectively.
  
4. A was then added to  $L_P$ :  $L_{PA} = A + L_P$ 
  - i) 112.2 dB
  - ii) 115.3 dB
  - iii) 110.0 dB respectively.
  
5.  $L_{PA}$ 's were summed:  $S = (L_{PA_i} + L_{PA_{ii}}) + L_{PA_{iii}}$ 

$$S = (112.2 + 115.3) + 110.0$$

$$S = 117.0 + 110.0 = 117.8 \text{ dB.}$$
  
6. In order to calculate the geometric attenuation, the straight line distance from the source to the microphone was figured from the scale diagrams of the L-shaped street. The attenuation was
 
$$B = 16.2 \text{ dB.}$$
  
7. B was added to S and the total summed level of the transient source effective at one foot was found to be

$$L_{PT} = S + B$$

$$= 117.8 + 16.2 = 134.0 \text{ dB.}$$

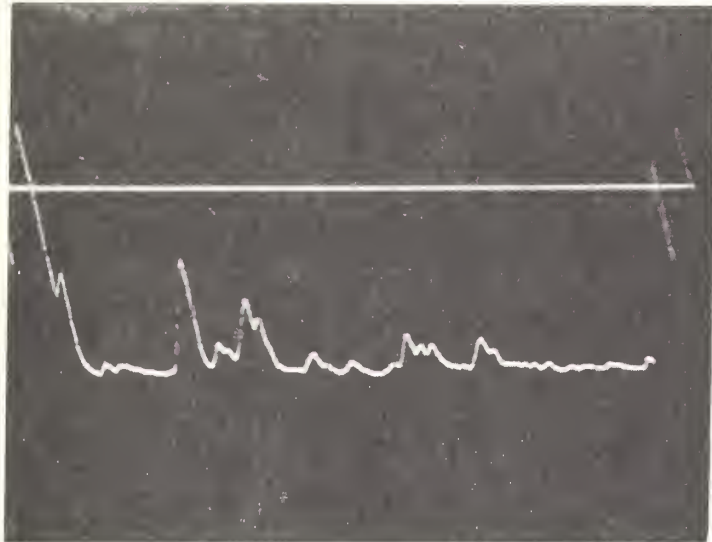


Fig. 22. Measured Value of Sound Pressure Level at 1 Foot (32 KHz Octave Band). Horizontal Time Scale 1 cm = 1 millisecc. Straight Line Represents 124 dB.

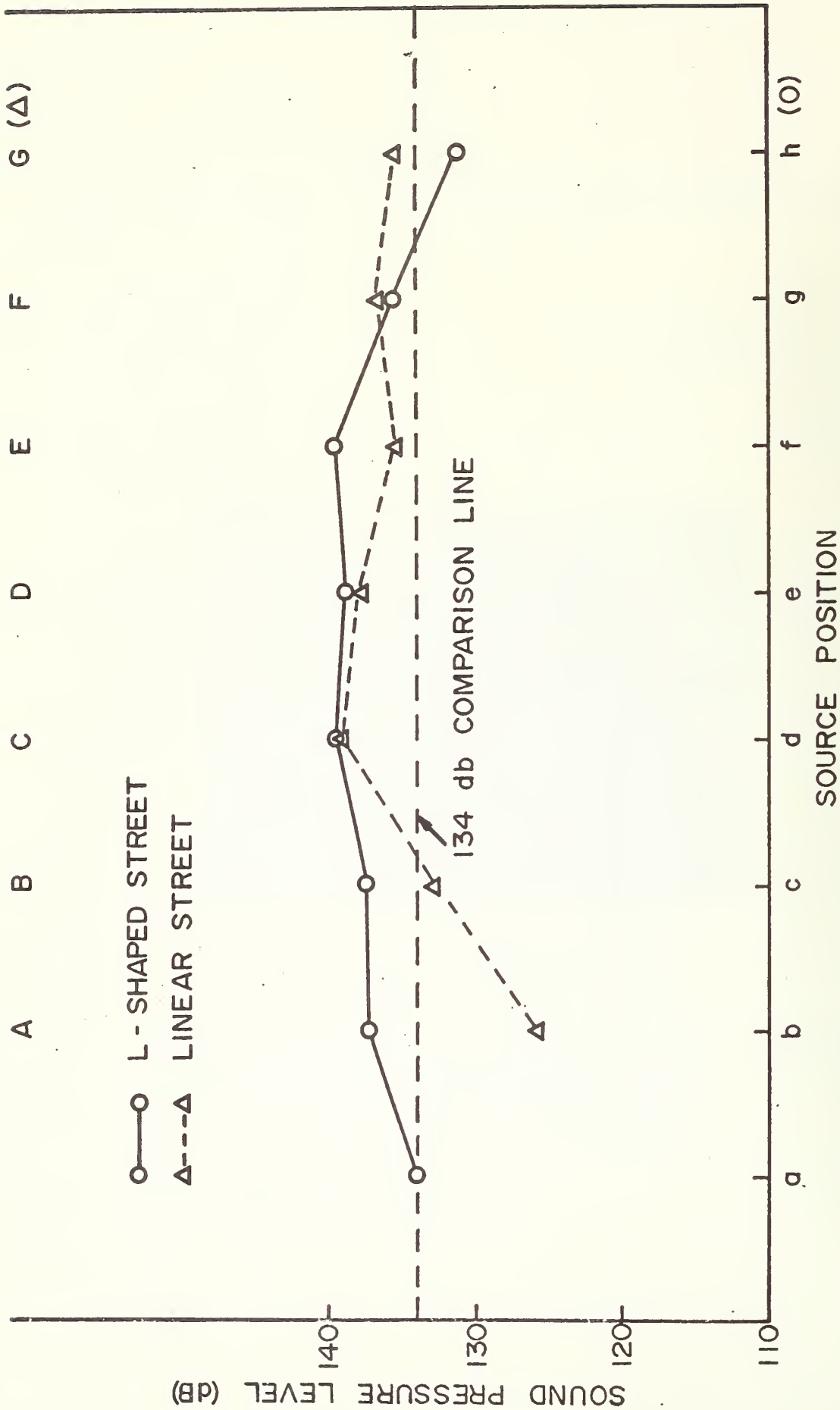


Fig. 23. Graph of  $L_p$  vs. source position.

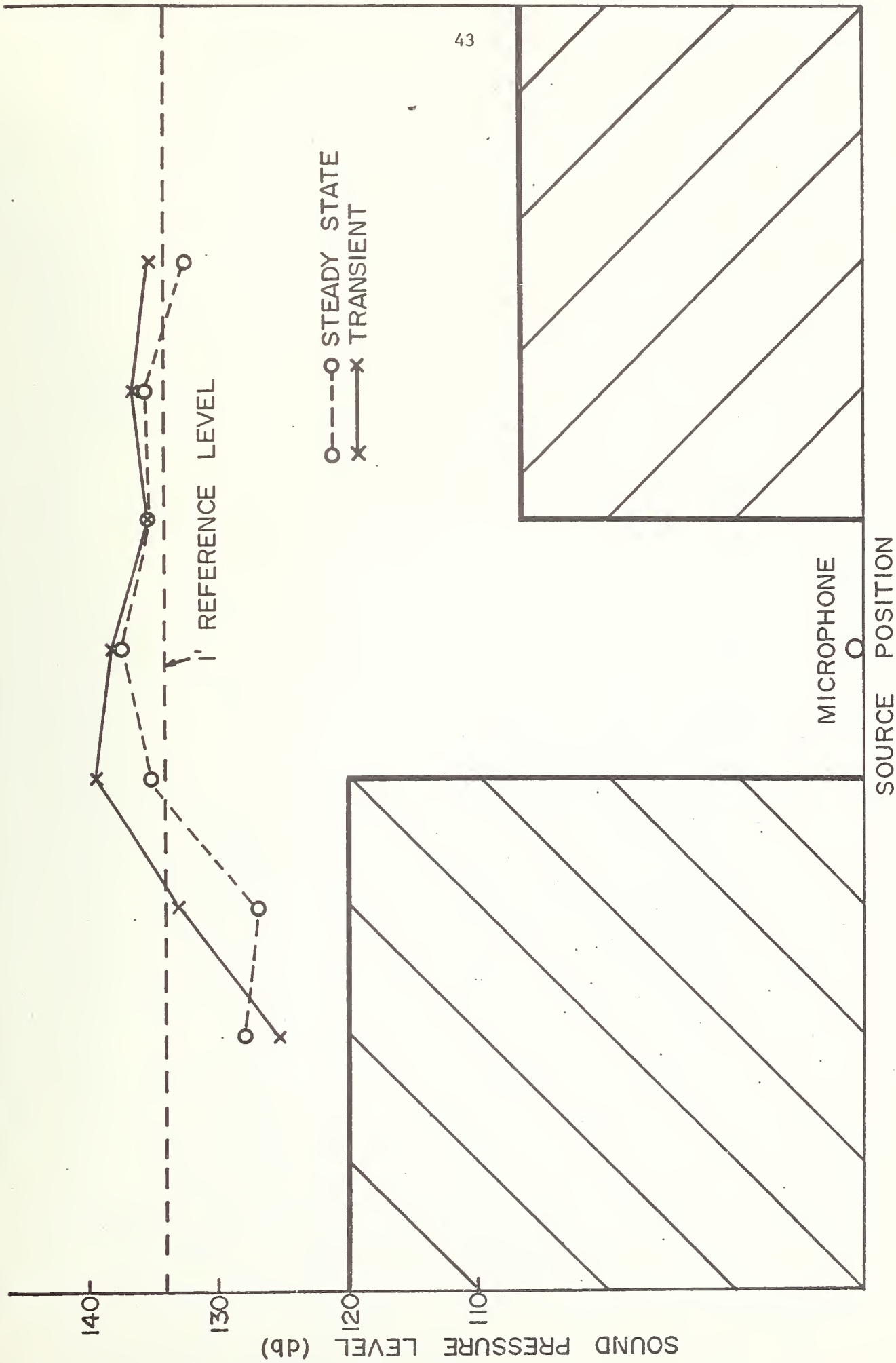


Fig. 24. Combined graph of  $L_p$  vs. source position for steady-state and transient sources.

As an illustration, consider data for the L-shaped street. For source position "a" indicated in Fig. 25, the straight line distance from source to microphone is 6.63 feet. From the transient data in Fig. 20 it appears that the bulk of the energy arrives 8 milliseconds after the source operates which corresponds to a propagation path of 9 ft (taking the speed of sound = 1127 ft/sec). This effectively means that the TG is increased. The geometric attenuation changes by 2.6 dB and the air attenuation in the 32 KHz band changes by 0.8 dB. Thus, the TG is increased by 3.4 dB.

The transient data can therefore be used to evaluate certain parameters that are necessary for calculating TG from the steady-state data. In that sense, the transient experiments are more than just a "check" on steady-state experiments, but in fact supply information that is necessary for the interpretation of the steady-state data.

#### Recommendations for Following Efforts

We believe that the work reported here allows us to recommend that certain areas of work be carried out, and to expect with some confidence that the results will be successful. We have three specific areas of work in mind, each of which is discussed in some detail in the following. They include the use of models to simulate larger urban sections, the application of modeling procedures to the needs of planners, and the use of model data as a guidance for field studies of noise propagation.

In the studies we have reported, the source is relatively close to the street where noise measurements are being made. Such a situation is pertinent to streets that are very close to the Verti- or Stol-port. In several Stol-port studies, however, the nearest residences are of the order of 1/4 to 1/2 mile from the flight path. Noise exposure at these sites

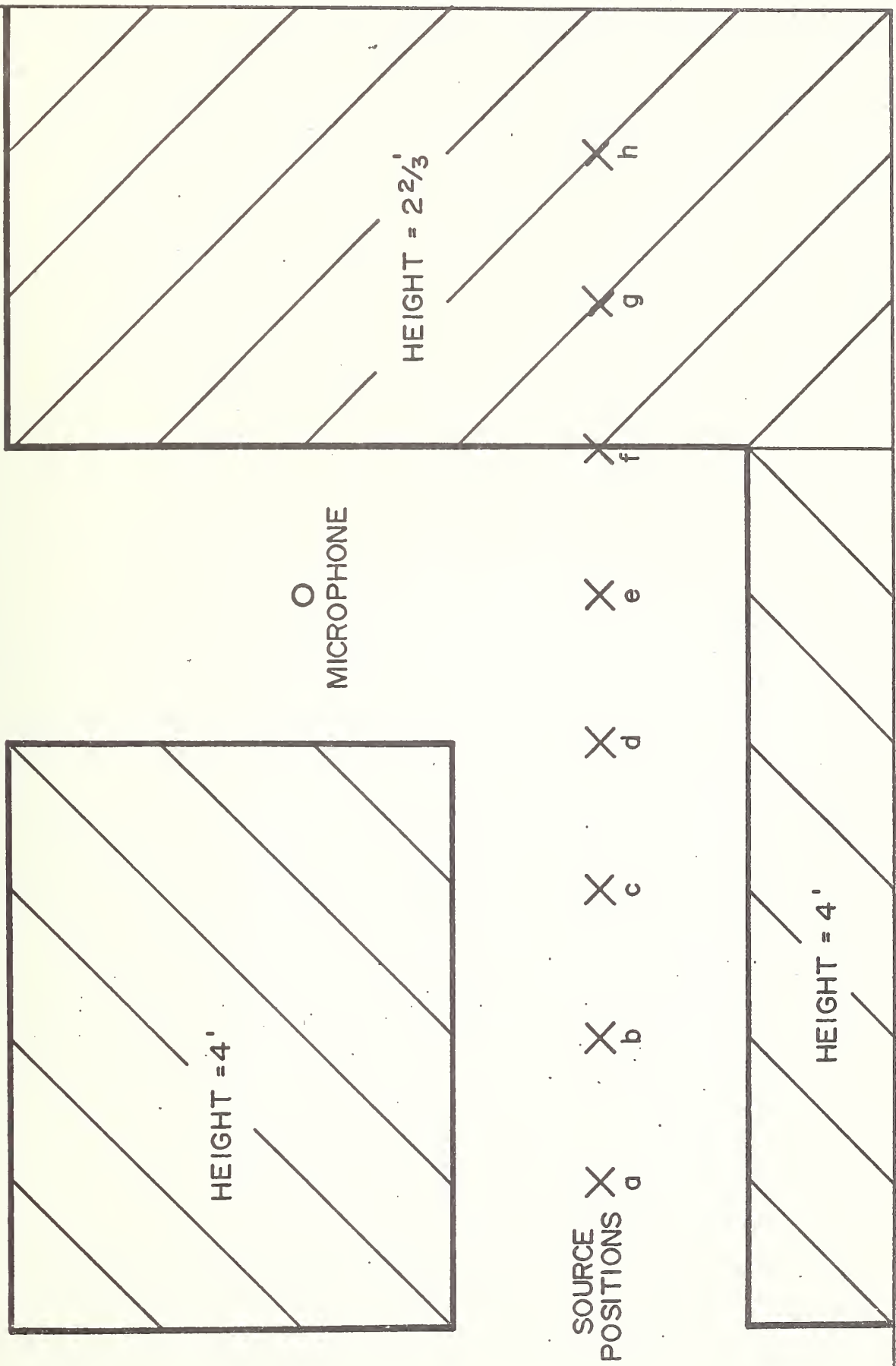


Fig. 25. Top view of L-shaped street model.

will be principally affected by channeling of sound along the streets, as discussed in Sections III and IV. It is important to know whether the net effect of the buildings and streets in this instance is to increase sound levels by channeling and reverberation, or to diminish them by shielding.

As mentioned in Section II, modeling the attenuation due to air absorption requires that we match the full-scale attenuation per wavelength. As a practical matter, this requires that we dry the air, getting the relative humidity down to less than 10%. The scale model of the urban area, constructed to 1:64 or 1:32 scaling, should be constructed in a box, as shown in Fig. 27, with a plastic cover to allow control of the atmosphere. The sound attenuation should be measured with varying numbers of buildings present, in varying density, orientation, etc. Our studies thus far indicate that the instrumentation we have been using should be directly applicable to such an experiment.

The experiment shown in Fig. 26 is one example of the use of the modeling instrumentation and techniques that we have been developing. Such an experiment is in effect a planning aid, since it allows one to assess the changes in noise impact that might result by a change in flight paths, building layout, topography, or airport location. Further experience with these procedures may be expected to lead to an experimental system that is simple enough to be given to planning personnel to be used in much the same way as optical procedures have been used in the past by architects for acoustical evaluation of auditoria.

Finally, models can be used as a helpful bridge between mathematical analyses of propagation and field studies of situations that approximate the mathematical assumptions. Due to logistic problems of field experiments

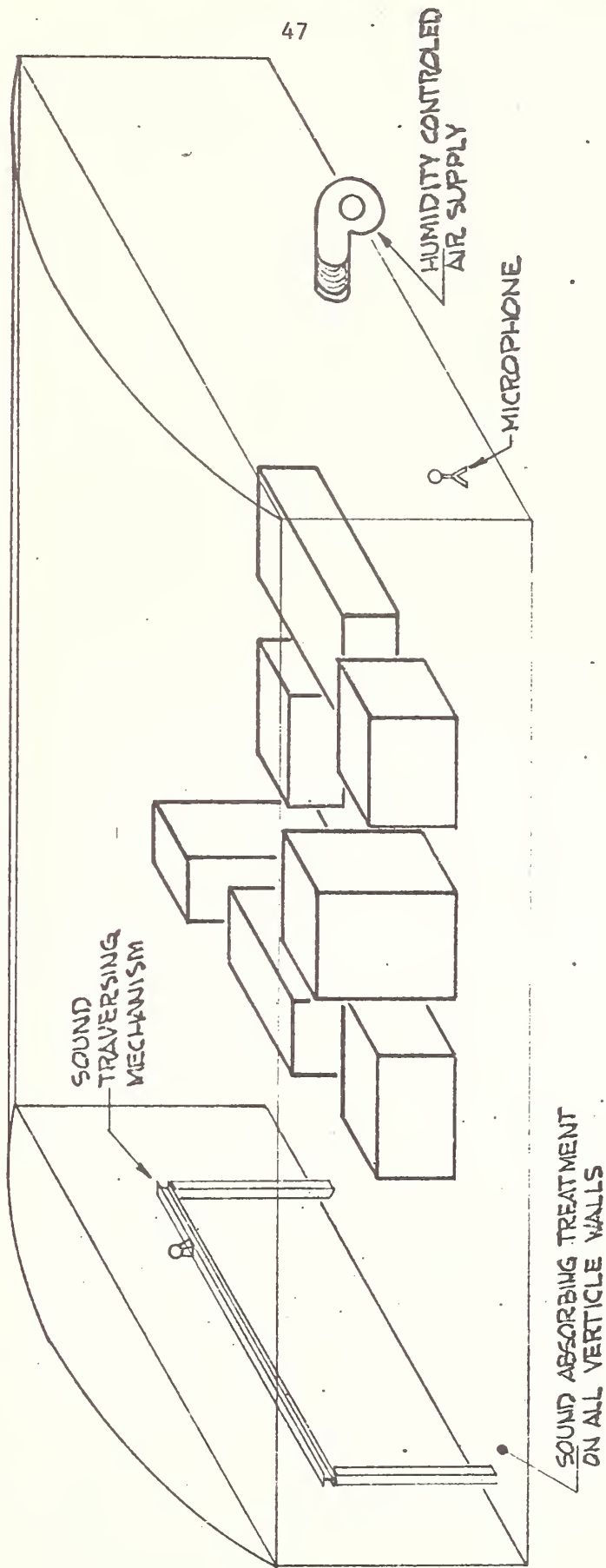


Fig. 26. 1:64 scale model of urban area near STOL-port.

however, the number of different locations and the variations at a given location that can be studied are limited. Model studies can simulate the very idealized mathematical assumptions quite well, and the model can then be varied in a "continuous" way to achieve the non-ideal conditions of the field experiment. In this way, one can examine the sensitivities of results to certain assumptions made in the mathematical analysis, and the adequacy of the parameters retained in the experimental model in determining important features in the field situation.

In summary, we feel that model procedures have a great deal of importance for many aspects of environmental noise propagation and control. We hope that the results shown in this report will lead others to similar conclusions.

## References

1. M. Delaney "A Note on the Effect of Ground Absorption in the Measurement of Aircraft Noise" J. Sound Vib. 16, no. 3, pp 315-322 (1971).
2. S. Auzou, Centre Technique et Scientifique du Batiment, Paris. Personal Communication.
3. L.B. Evans and L.C. Sutherland "Investigation of Anomalous Behavior of Sound Absorption by Molecular Relaxation" Wyle Laboratories Technical Memorandum 70-4, May 1970.
4. J.E. Piercy "Comparison of Standard Methods of Calculating the Attenuation of Sound in Air with Laboratory Measurements" Oral paper presented at 82nd meeting of Acoustical Society of America, October 21, 1971.
5. P.A. Veneklasan "Model Techniques in Architectural Acoustics" J. Acoust. Soc. Am. 47 no. 2 (part I) pp 419-423, February 1970.
6. J.E. Marte and D.W. Kurtz "A review of aerodynamic noise and propellers, rotors and lift fans" JPL Technical Report 32-1462, pp 33-34.
7. L.L. Beranek "Criteria for Noise and Vibration in Buildings and Vehicles", Noise Reduction, Chapter 20, ed. by Beranek, L.L., (McGraw-Hill Book Co., Inc., New York, 1960) pp. 530-533.
8. S.O. Rice "Mathematical Analysis of Random Noise" Contribution to Noise and Stochastic Processes, ed. by Wax, N. (Dover Publications Inc., New York, 1954) section 2.6.



HE 18.5  
A38  
no. DOT-TSC-93-1

BORROWER

Form DOT F 17  
FORMERLY FORM



DOT LIBRARY



00351909